Evaluation of monitored natural attenuation as a bioremediation technique of benzene in the "Bois Saint-Jean" site

Auteur : Emmanuello, Luca
Promoteur(s) : Brouyère, Serge
Faculté : Faculté des Sciences appliquées
Diplôme : Master en ingénieur civil des mines et géologue, à finalité spécialisée en géologie de l'ingénieur et de l'environnement
Année académique : 2022-2023
URI/URL : http://hdl.handle.net/2268.2/18355

University of Liège - Faculty of Applied Sciences

within a dual degree programme with

Alma Mater Studiorum – University of Bologna

Academic year: 2022-2023

_____

Evaluation of monitored natural attenuation as a bioremediation technique of benzene in the "Bois Saint-Jean" site

_____

Author:

Luca EMMANUELLO

Supervisor:

Prof. Serge BROUYÈRE

Co-supervisor:

Prof. Fabio FAVA

Master of Science in Geological and Mining Engineering

Master in Environmental Engineering, curriculum Earth Resources Engineering

Table of contents

1. General context

The Bois Saint-Jean site has been a subject of concern and investigation for several decades, stemming from its historical use as a slag pit for the steel industry and an illegal landfill for municipal and industrial waste during the 20th century. In 1999, the Walloon government entrusted SPAQuE with the task of characterizing and studying the site's requalification.

The primary goal of the investigations carried out by SPAQuE was to understand how the contamination at Bois Saint-Jean evolved over time and to assess whether the persistent pollutants concentrations posed any risks to human health or the environment. To achieve this, various characterization studies were conducted, identifying different zones within the site based on their geological and historical characteristics.

The focus of this thesis is on the South-West zone of Bois Saint-Jean, where benzene concentrations exceeding the thresholds set by the Walloon Soil Decree have been detected. Benzene (C_6H_6) is the first component of the BTEX group, known for its high toxicity and carcinogenic properties, making it of particular concern in the site's remediation efforts. Leaching from the landfill, facilitated by meteoric waters, was identified as the primary pathway responsible for groundwater pollution at the site.

Continuous monitoring by SPAQuE has been instrumental in understanding the groundwater dynamics at Bois Saint-Jean. The groundwater monitoring network comprises piezometers drilled during previous investigations or rehabilitation work.

The concentration of benzene in the area of interest exhibited erratic behaviour, making it difficult to pinpoint the exact source of the pollution. This hotspot is of particular concern due to its proximity to a walking area and the extended Liège Science Park.

To address the contamination issue effectively, two major remediation techniques have been implemented in the South-West zone: soil excavation and backfilling with clean soil, as well as in situ chemical oxidation (ISCO) using a product containing sodium persulphate.

The aim of this thesis is to assess whether implementing Monitored Natural Attenuation (MNA) is a viable remediation technique to ensure that the area is in safe conditions. The hypothesis is that microbial activity present at the site may be capable of reducing the remaining contamination following previous remediation works.

This study is built upon the foundation laid by a previous master's thesis, which investigated microbial degradation of residual benzene after ISCO remediation. This thesis aims to understand the changes in biodegradation parameters and assess the capacity of microbial activity to effectively reduce benzene concentrations. Specifically, the goal is to determine the existing biodegradation activities, such as nitrate reduction and sulphate reduction, and evaluate their significance in the natural attenuation processes occurring at the site.

The ultimate objective is to ascertain whether these microbial activities are capable of adequately mitigating pollutant levels to ensure human safety by assessing the potential of natural attenuation processes as a remediation strategy for the benzene contaminated area in Bois Saint-Jean.

This thesis has been developed based on my curricular internship experience at SPAQuE, where I had the opportunity to gather data first-hand and collaborate with experts in understanding the study's progression. During my internship, I actively participated in data collection efforts and worked closely with the team to comprehend the appropriate methodologies for conducting the study. The knowledge and practical experience gained from this internship have been instrumental in shaping the foundation of this thesis, allowing for a comprehensive analysis of the subject matter.

2. Site overview

2.1. Location

The site "Bois Saint-Jean" is located in the territory of the municipality of Seraing (Ougrée), 5 km at South-West far from the municipality of Liège. It covers the right side of the Meuse valley with an extension of 146,3 ha within the Seraing-Chênée region.

The site is at the centre of a triangle constituted by the city of Ougrée at North-West, the railway yard of Kinkempois at North-East, the University domain of Sart-Tilman at the South (SPAQuE, 2017).

The area is limited (fig. 2.1):

- at North, by the steel industrial conglomerate of Cockerill and the southern side of the Meuse river valley
- at South, by the Liège Science Park and the University domain of Sart-Tilman
- at East, by the Renory creek
- at West, by the Biez-du-Moulin creek.
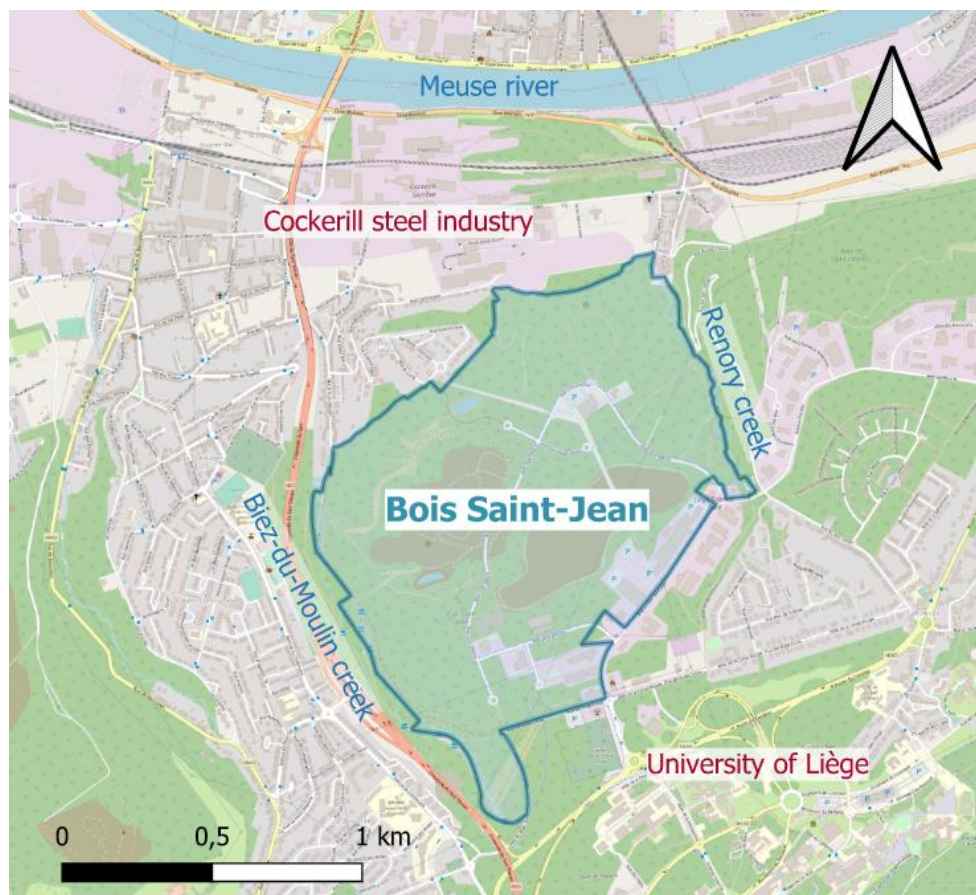
Fig. 2.1. Bois Saint-Jean area limits

2.2. Regional geology and hydrogeology

The Seraing-Chênée region has a relatively irregular topography. The valley bottoms are located between 60 and 80 m above sea level, whereas the southern plateaus of the region reach altitudes of 250 m.

The area is located between two hydrogeological basins (fig. 2.2a):
- Meuse basin, at the north, with a relatively wide alluvial plain, between 800 and 1500 m
- Ourthe basin, at the east, with a much narrower alluvial plain, between 110 and 340 m.

The topographic map of Bois Saint Jean reveals a distinct pattern of elevation, characterized by a gradual decrease towards the Meuse basin in the north and west boundaries, with the lowest altitude reaching as low as 80 meters. The central part of the region is predominantly around an elevation of 200 meters, while a notable increase is observed towards the southwestern region, where altitudes reach as high as 250 meters (fig. 2.2b).
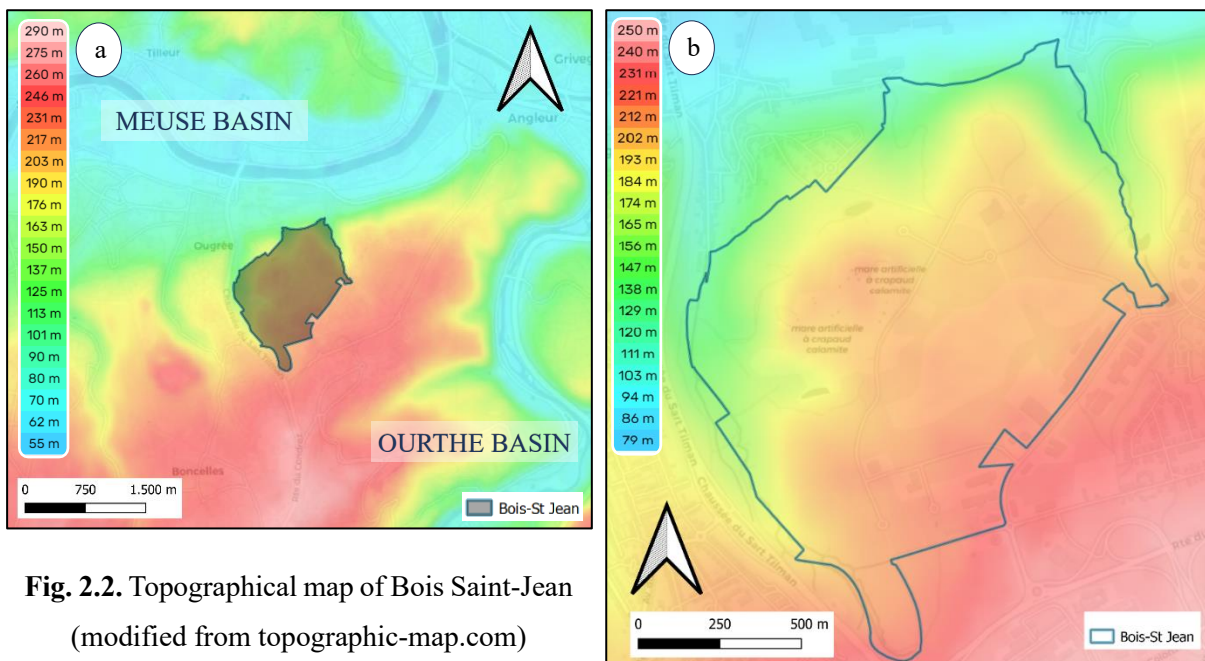
Fig. 2.2. Topographical map of Bois Saint-Jean (modified from topographic-map.com)

The Bois St-Jean area's bedrock primarily consists of Lower Devonian formations, which are part of the northern flank of the Dinant Synclinorium (SPAQuE, 2017). Over time, the folded and faulted Palaeozoic bedrock underwent extensive erosion, resulting in a flattened surface. On this surface, Oligocene (Tertiary) sediments were deposited, mainly comprising sandy deposits resting upon layers of flintstone from the Cretaceous period (ECOREM, 2000).

Additionally, the Oligocene deposits are covered by layers of gravel and occasional clay, with the latter however absent in correspondence of the site of interest (SPAQuE, 2003).

The region's prevailing soil type is a mixture of stones and loam with a schistosandstone or sandstone base, ensuring moderate to favourable natural drainage. Nonetheless, towards the very south of the site, the soil transitions to silty soil, which exhibits distinct drainage characteristics and water-holding capacity (fig. 2.3).
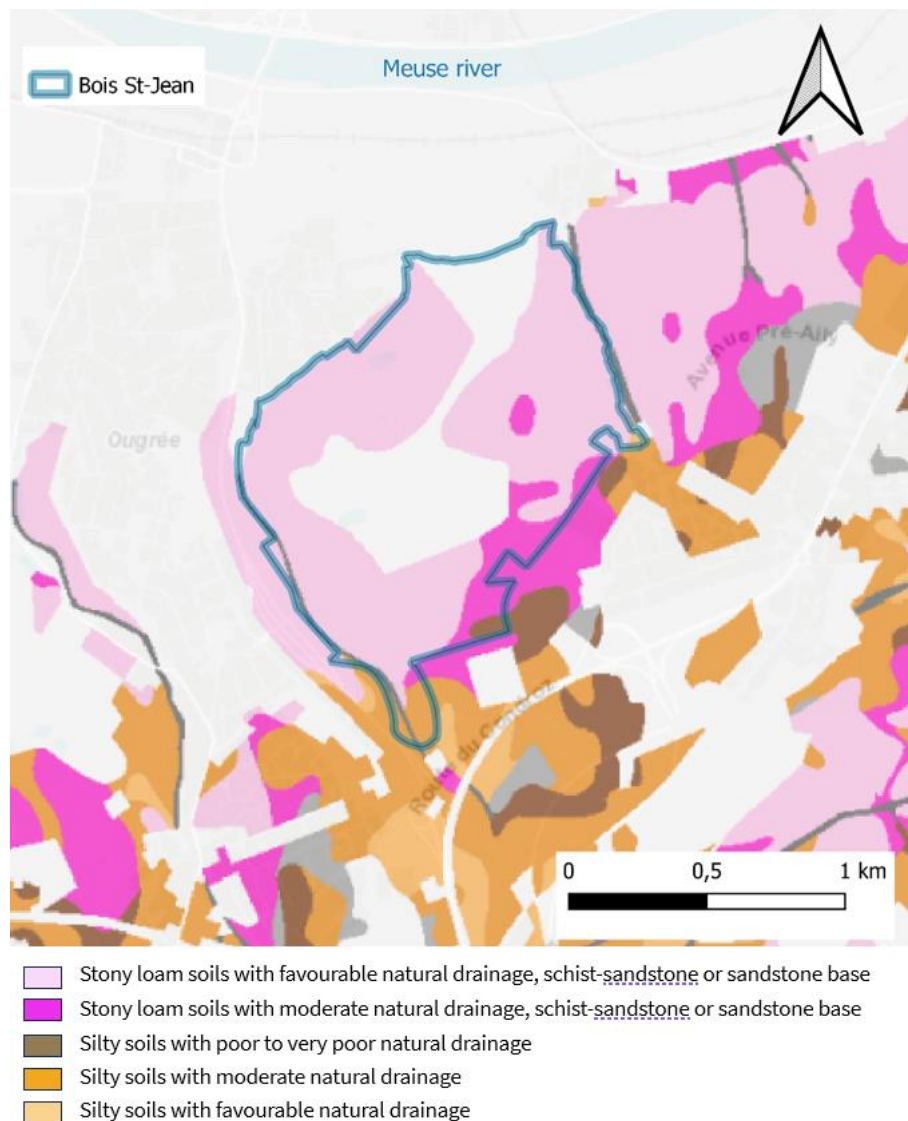
Fig. 2.3. Type of soil around Bois Saint-Jean (modified from WalOnMap)

The Oligocene sands in the area are particularly noteworthy for their significant aquifer potential, especially in regions with large deposits. However, the presence of Quaternary silts plays a crucial role in protecting the underlying aquifers. During periods of high rainfall, temporary perched water tables may be found (Ruthy et al., 2016).

The water resources of the Seraing-Chênée region are essentially located in the alluvium of the Meuse, in the limestone of Chaudfontaine-Embourg and in the chalk of Hesbaye. The schisto-sandstone terrains of the Houiller and the Middle and Lower Devonian comprehend:

- the aquitard with aquifer levels of the Lower Devonian: globally not very permeable micaceous sandstones and shales but with nevertheless potentially exploitable aquifers on a local scale

- the aquifer with aquiclude levels of the Lower Devonian: the alternation of sandstone and Devonian shale induces an alternation of aquifer levels with interesting potentialities (SPAQuE, 2017)

- The sketch of the hydrogeological cross-section in the Seraing-Chênée region illustrated below (fig. 2.4) is traced around 1 km south-west from Bois Saint-Jean, which in linear distance is between Ougrée and Boncelles.
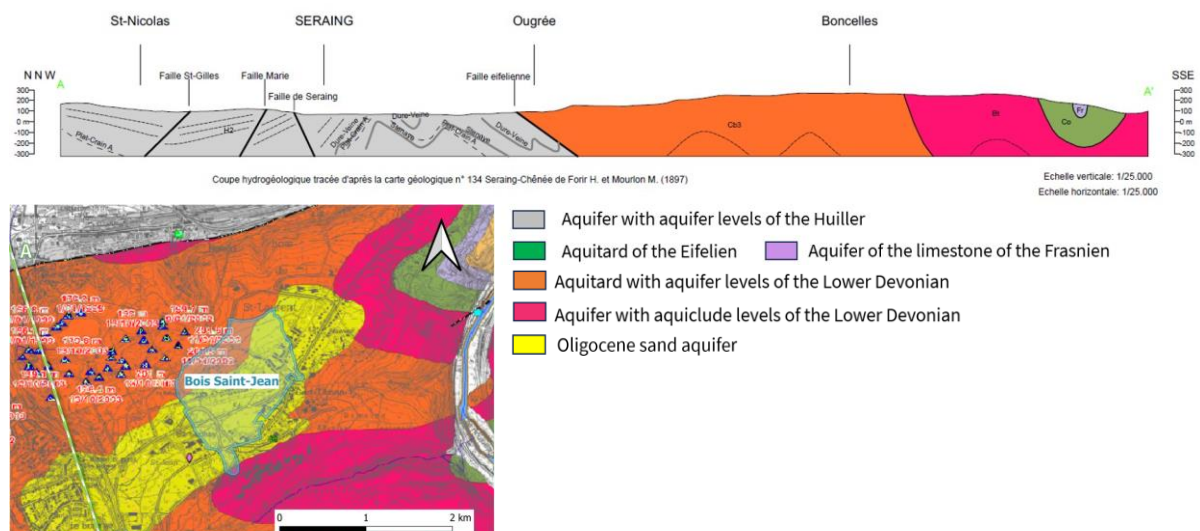
Fig. 2.4. Hydrogeological cross-section in Seraing- Chênée
(modified from *Carte Hydrogéologique de Wallonie*, Seraing Chenéè 42/5-6, 2015)

2.3. Local geology and hydrogeology

The site "Bois Saint-Jean" can be divided in different zones based on the topography, vegetation and soil composition. The benzene contaminated area is located within the southern side of zone 6, which corresponds to the south-west of Bois Saint-Jean according to a former ECOREM division (fig. 2.5).

This area records an elevation ranging from 180 m in the north to 215 m in the south and it covers approximately 12.9 ha. Within this section, there was a significant microrelief, partly due to the original topography and because of varying amounts of dumping and the presence of large blocks and debris, some reaching up to 2 m^3 in size (ECOREM, 2000).
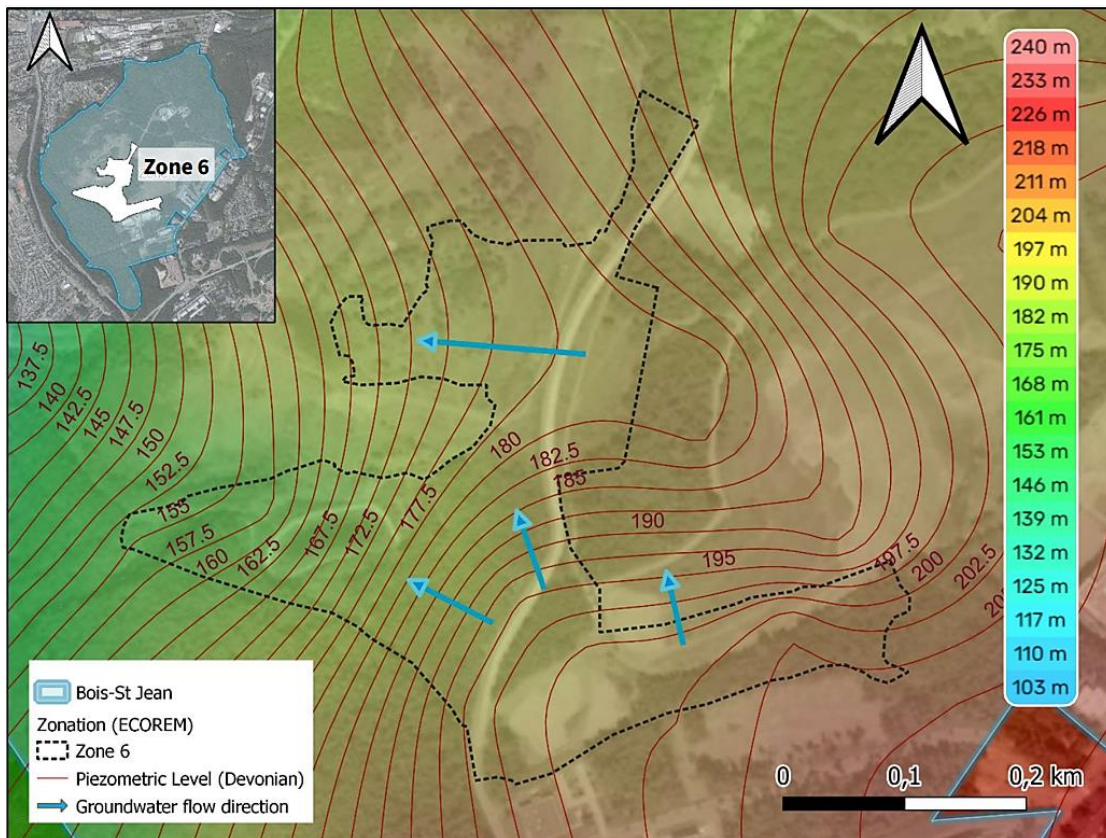
Fig. 2.5. Topographic and piezometric map of zone 6 (modified from topographic-map.com)

The vegetation consisted of shrubs, grass and trees, primarily birch and conifers. However, in correspondence of the contaminated area, the vegetation has been cut off during the implementation of the remediation works.

In proximity of the site, the Devonian bedrock appears not to be covered by Quaternary fluvial gravels. Due to the significant weathering of the shale, the bedrock is covered by at least a few meters of weathered material and Quaternary sediment deposition (Lox, 2023).

7

The investigations conducted by ECOREM (2000) and SGS (2002a; 2002b; 2003) indicate that the "Bois Saint-Jean" site is characterized by the following lithological sequence:

- Controlled backfill material, with thickness ranging from 0 to 28 m
- Compact red weathered clay, with thickness ranging from 0 to 3 m
- Red-greenish shales and grey-violet sandstones, more or less weathered, with localized presence of brown-yellow and black sands in the western part of the site.

The thickness of the weathering layer on the shales and sandstones is significant, reaching several meters of depth. Sandstones and shales are only exposed in the deep gorges carved by the Biez-du-Moulin and Renory streams.

Hydrogeological investigations conducted by SGS (2002a; 2003) have concluded on the presence of a single aquifer at the site, housed in the fractured and weathered Lower Devonian sandstone horizons. No aquifer has been observed in the backfill material.

The aquifer of the Lower Devonian sandstones and shales is observed at depths ranging from approximately 1 to 5 m below ground level, except in the backfill areas where it can be observed up to approximately 24 m below ground level. The natural outlets of the aquifer are the Biez-du-Moulin stream to the west and the Renory stream to the east, following the groundwater flow direction sketched based upon the piezometric level of the area (fig. 2.5).

Groundwater flows are also influenced by the presence of a former draining valley (Vieux Moulin stream) coming from the south and crossing the site beneath the slag heap. SGS investigations have also determined that groundwater circulation at the site occurs mainly within the natural terrain and is minimally influenced by the backfill material.

Slug tests and pumping tests conducted on the site have estimated the hydraulic conductivity of the Lower Devonian rocks to be approximately 10^{-5} m/s in the fractured sandstone horizons, while it is two order of magnitude lower in the compact upper layer made of shale and sandstone (SPAQuE, 2017). Slug tests performed within zone 6 indicate that the local conductivity values can range from 4.8 x 10^{-6} m/s to 2.5 x 10^{-4} m/s (Hallberg, 2021).

2.4. History of the site

A report drafted by SPAQuE provides an extensive overview of the activities performed within the site of Bois Saint-Jean, explaining how the site has been polluted over the decades, mainly as an illegal landfill (SPAQuE, 2022).

2.4.1. History of Bois Saint-Jean contamination

- **1905** - The Bois Saint-Jean becomes property of the SA d'Ougrée-Marihaye. It is immediately used as a location to establish an initial industrial waste slag heap, northeast of the site. Two rack railway lines are put into service between the Ougrée-Marihaye steel plant and the Bois Saint-Jean for pushing slag-carrying wagons. The slag was eventually dumped on the hillside, at the location of the original slag heap. It is also possible that, from this time, the Bois Saint-Jean was used as a timber reserve for mine support production and was consequently exploited

- **1935, 1941**, and **1942** - The Provincial Government authorizes the SA d'Ougrée-Marihaye to dump industrial waste on the Bois Saint-Jean site

- **1944-1945** - The site is repeatedly hit by targeted bombings and an aircraft also appears to have crashed directly or in close proximity to the rack railway line

- **1949** - The use of the rack railway line is abandoned, and it is subsequently dismantled.

- **1951** - The Municipality of Ougrée requests permission to establish a waste disposal site at Bois Saint-Jean, on the Ougrée-Marihaye slag heap and receives authorization for a period of ten years

- **1973** - The Belgian Society of Azote, Tensia (surfactant detergent powders), Air Liquide, La SA des Tubes de la Meuse, Isobelec, Linalux, Phénix Works, and the Municipality of Ougrée are said to be authorized by SA Cockerill to regularly dump waste on the site

- **1976** - Household waste, washing sludge from the two blast furnaces, and solid and liquid residues from the chemical industry are estimated to be dumped at the site annually, totalling 24000 m^3

- **1987** - A regional executive order regarding landfills puts an end to the waste dumping at the site

- **1994** (August 26 and December 7) - The DPE records illegal dumping (between fifty and one hundred cubic meters) of soil, inert waste, green waste, and household bulk waste at the site

- **1999**: A collection drain is installed north of the western slag heap to collect percolation water and direct it to the existing drainage system (stream to the west). In January-February, ISSeP reveals the presence of degraded containers of hydrofluoric acid, solvent drums, and bluish soils on the site. The heterogeneous soil consists of shales, slag, various fill materials, and soils with a strong odour of hydrocarbons. West of the site, the black slag exceeds 80°C at one meter below the surface, and fumaroles emerge from drill holes. ISSeP concludes that the site is heavily contaminated with heavy metals (As, Cd, Cr, Cu, Hg, Ni, Pb, and Zn) and various organic compounds.

2.4.2. Earlier remediation works

In 2000, the Municipality of Seraing acquired the site as part of the Sart-Tilman ULiège scientific park expansion. Later, an inventory conducted by SGS revealed various sources of pollution on the site, including slag, slag sand, steel mill ashes, domestic waste, metal bells, hydrocarbons, and cyanide.

The estimated volume of industrial waste exceeded 4 million m^3, while household waste amounted to half a million m^3. The volume of soil contaminated with hydrocarbons was estimated to be 82.000 m^3 (SPAQuE, 2022).

In 2002, the site rehabilitation efforts commenced alongside further characterization studies. The rehabilitation works carried out on the site were undertaken within the framework of a rehabilitation regional government decree (AGW) and funded by the European Regional Development Fund (FEDER) for the period 2000-2006.

The first phase aimed at rehabilitating the areas contaminated with cyanide. The works involved excavating the cyanide-contaminated soil and backfilling the excavated areas with clean soil.

The second phase (2003-2004) aimed at creating a controlled storage area (or confinement zone) on the areas corresponding to the former household waste landfills and the former hydrocarbon lagoon. The works included reshaping the waste mass, grouping scattered waste and contaminated soil into 'cells' on the surface of the site, installing an upper seal consisting of clay, an HDPE membrane, as well as a single layer of silt (1 meter thick) over the entire surface of the household waste landfills. Additionally, a layer of topsoil (30 cm thick), a peripheral drainage network to collect runoff water, and a drainage pipe to discharge the collected water to the Biez-du-Moulin stream were installed.

The third phase (2004-2005) aimed at securing the burning slag heap. The works began with levelling the slag heap to the natural terrain and extinguishing the excavated burning materials. They continued with the implementation of a biofiltering capping system (SPAQuE, 2006). Three years later, a wastewater treatment plant has been installed to collect and treat the significantly basic water leaching from the slag heap.

A fundamental step in the remediation of zone 6 of Bois Saint-Jean is the ISCO (In situ Chemical Oxidation) in 2020 by Suez. Although the former plan was to place 80 injection wells over a surface of 800 m^2, it was finally decided to perform a first campaign with 10 injection wells around 12 m deep, depending on the observations raised during their implementation, plus two monitoring wells P301 and P302 (fig. 2.6). In these 10 injection wells, a total of 3200 kg of PersulfOx has been equally distributed (Suez, 2020).
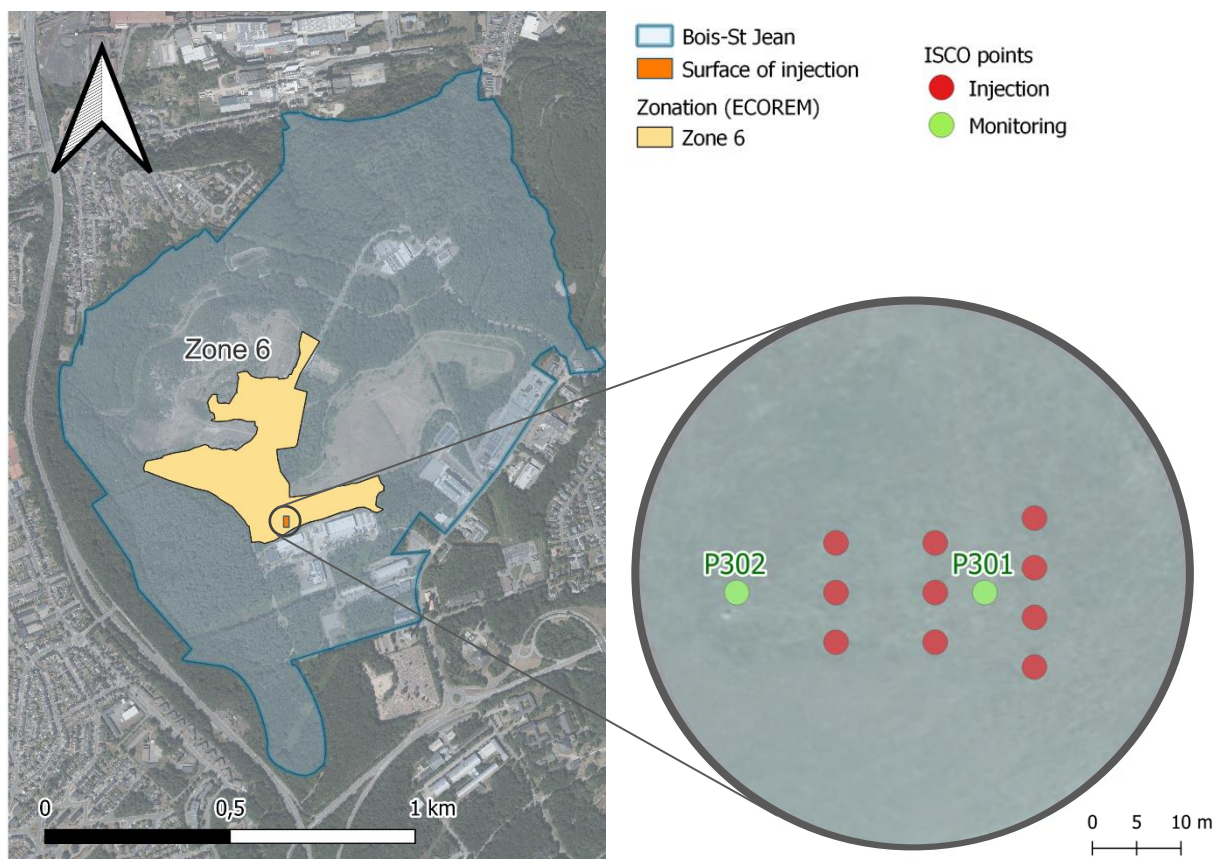
Fig. 2.6. Injection points of the ISCO remediation performed in 2020

This quantity was chosen by Regeneris, which claims this product to promote rapid and sustained in situ oxidation of a wide range of organic contaminants. PersulfOx contains a built-in catalyst that remains active through the entire lifespan of the persulphate oxidation reaction. Once the activating chemical is consumed, a level of radical formation is sustained as a result of the PersulfOx catalyst's persistence (Regenesis, 2018).

Sulphate free radicals are capable of degrading organic compounds to carbon dioxide and water. Degrading benzene by sulphate free radicals can be illustrated as the following reaction (Liang, et al., 2011):

$$16NA_2S_2O_8 + C_6H_6 + 12H_2O \rightarrow 6CO_2 + 30H^+ + 32Na^+ + 32SO_4^{2-}$$
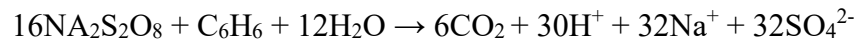
The generation of sulphate products in remediated site is evident from the major ions analysis and it is later discussed in Chapter 6. Compared to the sodium persulphate typical utilization procedure, PersulfOx is not activated with the addition of heat, hydrogen peroxide or base in order to generate sulphate radicals, thus resulting in a relatively safe and easy-to-use ISCO agent (Suez, 2020).

2.5. Land registry

In 1999, the site was acquired by SOGEPA from Usinor. Over time, various parcels of the site were sold to private companies, including an extension of the LIEGE Science Park. In 2007, SPAQuE became the owner of a portion of the site, while SPI obtained ownership of a section in 2013. The parts of the site sold by SPAQuE to SPI cover a major part of the mixed economic activity zone. In the sector plan, part of the site is located in a mixed economic activity zone and another in a green space zone (SPAQuE, 2017).

The extension of the LIEGE Science Park covers the central and southern areas of the site on the rehabilitated plots of land included in the sector plan as a mixed economic activity zone of economic activities (SPAQuE, 2020). These areas are served by a new road and all the necessary infrastructures (water, electricity, drainage, etc.) forming a large loop around the confined area. In the zone contaminated by benzene, once the area has been remediated, it is likely that SPAQuE will project a photovoltaic power plant.

3. State of the art

3.1. Bioremediation and Monitored Natural Attenuation

Bioremediation may be defined as the use of living organisms to remove environmental pollutants from soil, water, and gases. Organic compounds are metabolized under aerobic or anaerobic conditions by the biochemical processes of microorganisms (Collin, 2001).

The objective of bioremediation is to facilitate the complete degradation of hydrocarbons by microorganisms, resulting in the conversion of these compounds into harmless by-products, namely carbon dioxide and water. Bioremediation offers numerous advantages compared to conventional methods like landfill disposal, thermal and chemical treatments.

These advantages include the transformation of toxic waste into non-toxic substances, a more cost-effective or even cost-free approach to disposal, diminished health and ecological impacts, mitigation of long-term liabilities associated with non-destructive treatment techniques, and the capacity to conduct treatment directly at the site without excessively disturbing the native ecosystems (Sarkar et al., 2004).

In the field of environmental engineering, the bioremediation of contaminants can be achieved through an enhanced approach, namely consisting of bioaugmentation and/or bio-stimulation. The process of bioaugmentation involves the deliberate introduction of specifically cultured microorganisms into the contaminated system, aiming to degrade the specific contaminant. These cultures can either be obtained from the contaminated soil itself or sourced from a collection of microbes with proven capabilities to degrade the chemical of interest. Once introduced, these cultured microorganisms selectively consume the contaminants, thereby facilitating the remediation process.

On the other hand, the process of bio-stimulation involves the addition of supplementary nutrients in the form of organic and/or inorganic fertilizers into the contaminated system. This nutrient augmentation serves to enhance the population of naturally occurring microorganisms already present in the system. By providing these additional nutrients, the indigenous microorganisms experience an increase in their population, thereby promoting the degradation of contaminants within the system (Pankrantz, 2001).

The choice of an enhanced bioremediation approach in specific portions of the contaminated site could be driven by the need to effectively address the high concentration and upward trend of pollutants in those areas. On the other hand, across larger plume areas where contaminant concentrations are not considerable or increasing significantly, an intrinsic bioremediation (i.e., natural attenuation) becomes a feasible option (Key et al., 2022).

By utilising processes that occur naturally in the subsurface, natural attenuation may be an alternative site management concept to engineered intervention for specific, well-documented site circumstances, if it can achieve technical and regulatory requirements of reducing risks to acceptable levels within a reasonable time-frame (Alzarez & Illman, 2006).

The technical application of natural attenuation processes for the management of contaminated groundwater is termed 'Monitored Natural Attenuation' (MNA). The conceptual basis for natural attenuation is the exploitation of naturally occurring physical, chemical and biological processes that act within an aquifer to reduce contaminant mass, concentration, flux or toxicity (Carey et al., 2000).

Contaminated groundwater is transported from the source at A, through the plume B, to the receptor at C (Fig. 3.1). The success of MNA relies on achieving a significant reduction in flux and pollutant concentration measured across the control planes, thereby ensuring acceptably low risks at the receptor level.

Although abiotic processes such as dispersion, sorption and chemical reaction contribute to pollutant mass reduction through the natural attenuation of plumes, biodegradation is typically the most important as it results in the pollutant mass reduction through destruction or biotransformation of organic contaminants by in situ micro-organisms (Thornton & Rivett, 2008).

Microbial populations use terminal electron acceptors during respiration to breakdown and/or degrade dissolved organic constituents in groundwater. Oxygen is the most favourable electron acceptor followed by nitrate, iron, sulphate and then carbon dioxide (EPRI, 2004).

The conceptual model for intrinsic biodegradation typically notes the occurrence of aerobic conditions upgradient, outside the source and perhaps in the plume areas. The source area is typically anaerobic and depleted of oxygen whereas the plume area corresponds to reduced to depleted aerobic conditions. At the periphery or fringe of the plume, mixing between the plume and background groundwater triggers aerobic respiration, nitrate reduction, and sulphate reduction (EPRI, 2004; Thornton & Rivett, 2008).

Generally, degradation processes at the plume fringe are more important for attenuation than processes in the plume core, where slower anaerobic degradation by manganese reduction, rion reduction and methanogenesis can prevail (Thornton et al., 2001).
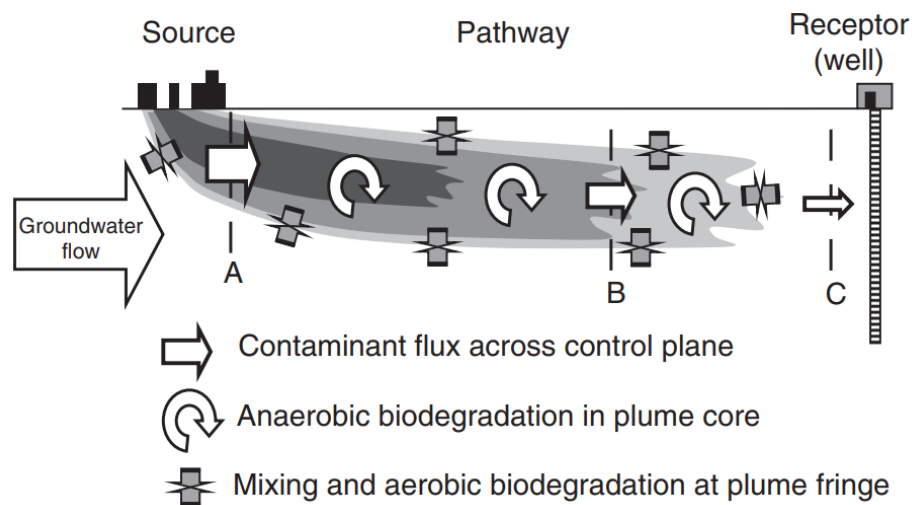
Fig. 3.1. Conceptual model for natural attenuation of biodegradable contaminants in groundwater (Thornton & Rivett, 2008)

When making a selection among suitable remediation techniques, factors associated with the potential advantages and disadvantages should be carefully considered. The table below (tab. 3.1) provides a summary of them with regards to the implementation of MNA:

Advantages	Disadvantages
Overall costs are lower than other techniques	Longer periods of time may be required to mitigate contamination
Minimal disturbance to the site operations	Natural attenuation is not appropriate where imminent site risks are present
Potential use next and below buildings	Despite prediction of stationary conditions, migration of contaminants may occur
Reduced risk of human exposure to contaminants near the pollution source	More efforts may be required to gain public acceptance of natural attenuation
Complete destruction of organic contaminants through biodegradation processes	Intermediates of biodegradation may be more toxic than the original contaminants
Stabilization of metals and metalloids	Some inorganic contaminants can be immobilized but not degraded

Tab. 3.1. Advantages and disadvantages of MNA (Balland-Bolou-Bi et al., 2022)

3.2. Endorsement of the Monitored Natural Attenuation

The implementation of MNA is relatively recent: The United States Environmental Protection Agency (US EPA) published definitions for the concept of natural attenuation in the 1999 OSWER (Office of Solid Waste and Emergency Response) directive regarding the use of MNA for the remediation of contaminated soil and groundwater. Knowledge concerning natural attenuation, as well as acceptance and application of MNA as a stand-alone technique or in combination with other treatments, has increased in the last two decades.

During this period, the application of MNA as a method for managing and remediating contaminated groundwater has sparked extensive discussions. Natural attenuation has sometimes been mislabelled as a simplistic "do nothing" approach to site remediation. However, it should be conceived as a "proactive approach" or "passive approach", in which the verification and monitoring of the processes of natural remediation relies on a meticulous evaluation process and necessitates a substantial commitment to long-term performance monitoring rather than merely on technical processes (Balland-Bolou-Bi et al., 2022; Thornton & Rivett, 2008).

Nonetheless, there have been differences as to how individual countries or regions within the European Union dealt with MNA within the framework of contaminated soil remediation (Declercq et al., 2012).

The jurisdiction for soil legislation in Belgium is the responsibility of the regions: Flanders, Wallonia, and Brussels Capital. Specific legislation for the remediation of contaminated soil in Wallonia dates from April 1st, 2004 (Décret relatif à l'assainissement des sols pollués). Within the framework of the 2008 Soil Decree, MNA is admitted among the remediation techniques (Halen et al., 2010). In the "guide de référence pour le projet d'assainissement" (GRPA), Code Wallon de Bonnes Pratiques V05 (applicable from 1st February 2023), the MNA "can be considered as a stand-alone technique for pollution with limited concentrations and it should be contemplated as an intermediate measure pending the clean-up of a site with high concentrations of pollutants" (SPW, 2008).

3.3. Assessment of the Natural Attenuation potential

In the pursuit of evaluating the natural attenuation potential at Bois Saint-Jean, valuable information can be captured from various sources of insight, encompassing hydrogeochemical characterization, isotope analysis, and microbial investigations. Each of these analytical approaches plays a crucial role in untangling the complex interactions between pollutants and the subsurface environment.

3.3.1. Hydrogeochemical characterization

Traditional investigations of groundwater have predominantly focused on monitoring changes in its chemical properties over time and space (Kennedy et al., 1999). Graphical representations like Stiff and Piper diagrams, combined with basic statistical analyses, have been the conventional tools for interpreting chemical analysis results (Lee et al., 2001).

To gain a more comprehensive understanding of the hydrogeochemistry of the groundwater system various physiochemical data, such as temperature, redox potential, dissolved oxygen, electrical conductivity, pH, and alkalinity, in addition to the concentration of chemical species like major cations and anions and chemical biodegradation indicators are incorporated.

The alteration of geochemical indicators during the interaction of pollutants with groundwater elements can provide valuable insights into the occurrence of hydrocarbon biodegradation and water-rock interactions (Kao and Wang, 2001). Furthermore, in situ parameters like redox potential and electron acceptor concentrations can offer hypotheses about the type and potential of biodegradation processes occurring.

The analysis of hydrogeochemical parameters also involves comparing the characteristics of the polluted piezometers with those of a reference piezometer that remains unaffected by contamination. This comparison enables to identify the specific electron acceptors that are being consumed during biodegradation processes or to assess the impacts of implemented remediation techniques, such as in situ chemical oxidation.

By studying the changes in the groundwater composition resulting from the injection of specific compounds during remediation efforts, it is possible gain valuable insights into the effectiveness of these techniques and their influence on the natural geochemical processes occurring in the aquifer.

Understanding the variations in electron acceptor concentrations and other key hydrogeochemical parameters is crucial for evaluating the potential of monitored natural attenuation as a suitable remediation approach and ensuring the safety and long-term sustainability of the site.

Traditional methods used to confirm bioremediation in the field have involved monitoring decreases in contaminant concentrations, electron acceptors, and increases in microbial byproducts (Borden et al., 2000). However, it can be a challenge to prove biodegradation in the field, since other processes such as volatilization, dispersion, and sorption can cause contaminant attenuation, and accurate mass balances are difficult to obtain (Davis, et al., 1999). For this reason, further evidence through other analyses is essential.

3.3.2. Isotope analyses

Isotopes can be defined as atoms of an element having different number of neutrons but same number of protons or electrons. Atoms which do not decay with time or take infinite time to decay are called "stable" isotopes.

Carbon, hydrogen, nitrogen, oxygen, and sulphur are the major elements of organic compounds. Furthermore, chlorine is a significant constituent of xenobiotic chemicals. These elements have at least two stable isotopes which can be distinguished mass spectrometrically (Meckenstock, 2004).

Although the chemical and physical properties of stable isotopes are nearly identical, slight differences arise from a quantum mechanical effect depending on different zero-point energies of the heavy and light isotopes. The higher zero-point energy of the lighter isotope means that a chemical bond formed by a lighter isotope is weaker than one by the heavier isotope (Bigeleisen & Wolfsberg, 1959).

This principle controls the reactivity of the individual stable isotopes in the environment and induces isotope fractionation. The extent of isotope fractionation during synthesis of organic compounds leaves a fingerprint in terms of isotope composition providing clues that may be used to identify sources, transformation reactions, and sinks of organic compounds in the environment (Meckenstock, 2004).

Isotope ratios in naturally occurring compounds vary due to kinetic isotope effects during their production which are understood as equilibrium isotope effects in processes without net

reaction (Kleikemper J. , et al., 2002). The common way to express the stable isotope ratios of a given compound is the deviation $\delta(‰)$ from an international standard:

$$\delta(‰) = \left[\frac{(R_s - R_r)}{R_r}\right] \times 10^3 = \left[\left(\frac{R_s}{Rr}\right) - 1\right] \times 10^3$$

where R_s is the isotope ratio of the sample and R_r the stable isotope ratio of the standard

Non-destructive natural attenuation processes such as dispersion, sorption, or volatilization frequently do not entail significant isotope fractionation (Slater et al., 2000). In contrast, chemical reactions and bio-transformations involve the formation or breaking of bonds and are therefore generally associated with isotope effects. (Bergmann et al., 2011).

This offers the possibility of assessing biodegradation at contaminated sites by analysing the isotopic composition of contaminants in field samples, either at one point over time or spatially resolved along the flow direction of a plume (Bergmann et al., 2011).

The analysis can be performed at a single point over time or spatially resolved along the flow direction of a plume. Compound-specific isotope analysis (CSIA) can be used to directly monitor biodegradation of aromatic hydrocarbons in groundwater. CSIA is based on the principle that molecules with light isotopes in the reacting bond, such as ^{12}C and ^{1}H, are generally degraded faster than those with heavy isotopes such as ^{13}C and ^{2}H. The result is a shift in the isotopic composition of the remaining contaminant pool as it becomes progressively more enriched in molecules containing the heavy isotopes (Ahad et al., 2000; Ward et al., 2000).

The isotopic data measured during biodegradation of aromatic hydrocarbons have been found to fit a Rayleigh isotopic model, which relates the initial isotopic composition of a substrate relative to the isotopic composition of the substrate at any given time point during biodegradation (Mariotti et al., 1981).

By evaluating experimental isotope data according to the Rayleigh isotopic model, enrichment factors (ε), which relate isotopic shifts to the extent of biodegradation (more negative values of ε indicate stronger fractionation), can be derived (Mariotti et al., 1981).

Enrichment factors determined during biodegradation of a compound generally vary as a function of biochemical pathway (Morasch et al., 2002). Under anaerobic conditions, biodegradation of BTEX compounds, such as benzene, is associated with a significant carbon and even more pronounced hydrogen isotope fractionation (Vieth, et al., 2005). The resulting isotopic fractionation may vary considerably as a function of terminal electron acceptor (Mancini et al., 2003).

3.3.3. Microbial analyses

Microorganisms, comprising bacteria, fungi, protozoa, and algae, constitute a substantial proportion of biomass within various ecosystems, including soil, groundwater, and the ocean. Among these ecosystems, soil harbors an immense microbial diversity, with numerous taxa present in each gram of soil. As a result, microorganisms play a crucial role in the degradation, transformation, and adsorption of contaminants, owing to their significant biomass and diversity (Alvarez-Rogel et al., 2021).

The processes by which microorganisms degrade or transform the contaminants are metabolic or enzymatic actions based on growth and cometabolism processes. The bacterial catabolic metabolism for hydrocarbon degradation can be aerobic or anaerobic. The concentration of oxygen affects degradation rates; in fact, under aerobic conditions, biodegradation is faster and more efficient because oxygen is the final electron acceptor. Under anaerobic conditions, the final acceptor of electrons can be nitrate, ferric iron, manganese or sulphate, and biodegradation is slower and if compared to degradation under aerobic conditions (Pandolfo et al., 2023).

Environmental conditions and microbial competition will ultimately determine which anaerobic biodegradation processes would dominate. In scenarios where oxygen levels are depleted and nitrate is available, facultative denitrifiers can utilize nitrate as electron acceptor to mineralize contaminants through denitrification. Subsequently, when nitrate in the aquifer becomes depleted, ferric iron becomes a viable electron acceptor. Aquifer sediments typically contain substantial amounts of ferric iron, offering a significant electron acceptor reservoir for hydrocarbon biodegradation.

Following the exhaustion of DO, nitrate, ferric iron and manganese, sulphate-reducing bacteria can degrade hydrocarbons by utilizing sulphate as the electron acceptor via the sulphate reduction process. If sulphate depletion occurs, methanogenic bacteria have the potential to biodegrade hydrocarbons using CO_2 as the electron acceptor (Kao et al., 2010).

It is of paramount importance to note that there are often key questions that are relevant to the natural attenuation performance assessment that cannot be answered using conventional microbiological and microcosm studies.

These include establishing which micro-organisms in a community containing many different populations are responsible for contaminant degradation, what function they have and under what conditions they are active. In fact, due to their complexity and variety, the removal of hydrocarbons from the environment cannot rely on a single species but requires versatile bacterial consortia (Alvarez & Illman, 2006).

Reproducing in situ conditions in laboratory microcosms can be difficult, even using native aquifer material and groundwater that has been carefully sampled at the site. Hence, biodegradation rates determined for contaminants in laboratory studies may not be fully representative at the field scale (Thornton & Rivett, 2008).

Traditional bacterial culture techniques have been fairly inefficient and slow to yield results. The potentials of many bacteria for aspects of remediation have often not become readily apparent due to such limitations. More recently, with the increasing speed of modern analytical techniques, such limitations are being overcome (Huang, et al., 2019).

In this sense, targeted sequencing of functional genes could provide information that directly codes for function and hence provides a functional framework for classification, and by inference, its host's taxonomic identity (Penton et al., 2013).

16S-rRNA targeted sequencing can be performed through polymerase chain reaction (PCR)-based techniques, which is a molecular technique that works by determining amplified target gene fragments (Cao et al., 2020).

Molecular (i.e., nucleic acid-based) techniques are preferred for environmental monitoring because they preclude laboratory isolation and cultivation of bacteria, which can be extremely time-consuming and often unsuccessful at including the majority of bacterial species in groundwater samples. Molecular techniques focus instead on catabolic genes that code for specific pollutant-degrading enzymes (Beller et al., 2002).

In fact, biodegradation initiates when diverse contaminant catalytic enzymes in microbes participate in the redox reactions. Parameters including the number of specific degrading microbes (i.e., microbial enumeration), the contaminants genotoxicity (i.e., mutagenicity), and the physiological activity, especially the abundance and expression level of corresponding degrading genes, reflect the biodegradation potential and efficiency (Cao et al., 2020).

The method, based on continuous measurement of the fluorescence signal during DNA amplification, allows rapid and precise quantification of target genes, resulting in a good potential in the quantification of specific biological functions in the environmental samples.

3.3.4. Lines of Evidence

By examining hydrogeological, chemical, and microbiological data, the occurrence and extent of contaminant attenuation processes can be systematically documented and quantified (Wiedemeier et al., 1999). The use of multiple 'lines of evidence' based on the analysis of groundwater quality and other data collected from contaminated sites is central in the assessment process for MNA. This approach plays a crucial role in determining the feasibility of MNA by employing a "weight of evidence" methodology.

In the technical protocols reviewed by Sinke (2001), the following lines of evidence can be considered:

1. Historical contamination data: entails showing a consistent decrease in contaminant concentration downgradient of the source along the plume flow path over time at adequate monitoring or sampling locations. The analysis should provide evidence that the reduction in concentration is not only attributed to processes associated with plume migration, such as dispersion and dilution. This line of evidence indicates the occurrence of natural attenuation but does not conclusively prove mass loss of contaminants (Alvarez & Illman, 2006).

2. Geochemical indicators: the objective is to illustrate the specific type(s) of natural attenuation processes occurring by analysing hydrogeological and groundwater quality data obtained from the site. The assessment is made by comparing changes in the concentration of the geochemical indicator species and other hydrogeochemical parameters in the samples from the plume and uncontaminated aquifer.

3. Additional laboratory or field data: using data such as microbiological analysis to demonstrate the presence and activity of indigenous micro-organisms able to biodegrade contaminants, identify the specific mechanism responsible for degradation and provide estimates of degradation rates, for interpretation of attenuation at the field scale (Thornton & Rivett, 2008)

4. Former investigations

4.1. Earlier investigations by SPAQuE

The extensive dataset provided by SPAQuE offers a valuable opportunity to conduct a comprehensive temporal evolution analysis of the sampling campaigns, with a particular focus on benzene, given its concentrations exceeding regulatory limits. The benzene concentrations were compared to thresholds set by the 2018 Wallonia Soil Decree in the Annex I.

This legislative framework, established by the Walloon Region of Belgium, serves as a comprehensive tool for managing soil and water contamination to safeguard both human health and the environment. The decree includes a set of guidelines and standards designed to regulate soil quality, outline procedures for evaluating and remedying contaminated sites, and ensure compliance with specific concentration thresholds for contaminants in soil and groundwater (SPW, 2018)

These concentration limits, referred to as Valorisation Soil (VS) thresholds, act as a benchmark to assess the extent of contamination and the efficacy of remediation efforts. For benzene, the VS threshold for groundwater is set at 10 µg/L, regardless of projected land utilization. By comparing benzene levels in groundwater against this established threshold, it is possible to determine if the regulatory requirements outlined in the 2018 Wallonia Soil Decree are met.

The table provided below (tab 4.1) presents the temporal evolution of benzene concentration in selected piezometers, which are localised as shown in the map (fig. 4.1).

Benzene concentrations [µg/L]						
Piezometer	18/07/2017	14/10/2020	19/11/2020	16/12/2020	03/03/2021	15/11/2021	26/07/2022
Pz12	<0,2	<0,2	<0,2	<0,2	<0,2	2,40	<0,2
Pz17		<0,2	<0,2	<0,2			
Pz18	3500	6	3,50	4,50	17	320	55
P230	<0,2	<0,2	<0,2	<0,2			
P301		130	1,90	39	170	7500	1100
P302		800	1300	320	54	89	0,75

The values in red exceed the 2018 Wallonia Soil Decree VS = 10 µg/L for benzene in groundwater

Tab. 4.1. Temporal evolution of benzene concentration
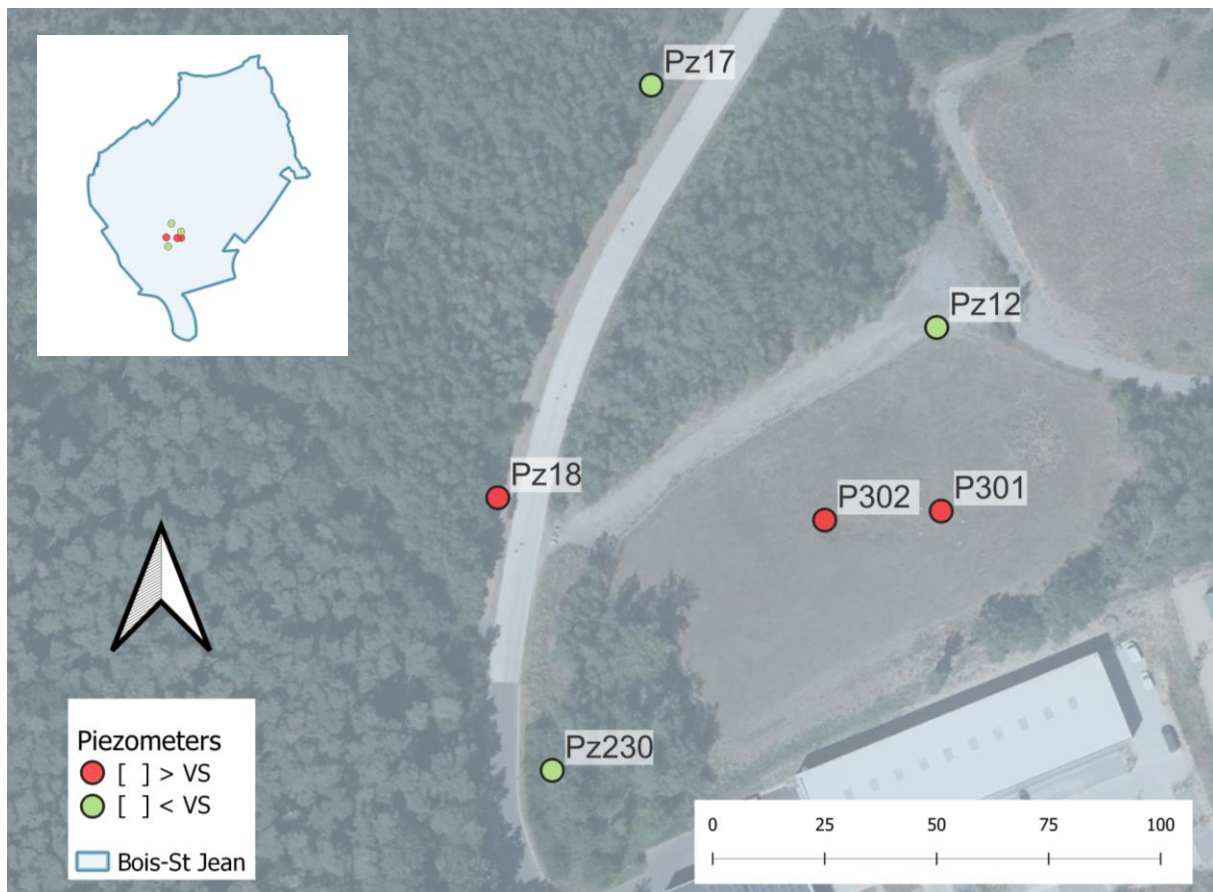
Fig. 4.1. Localization of the piezometers of earlier investigations

As depicted in the map, the plume of pollutants exhibits a horizontal extension, originating from the source area around P301 and following the groundwater flow direction towards the northwest. The delineation of the area of interest is evident from the concentrations that fall below the detection limit or remain below VS threshold.

Pz17 and P230 consistently exhibit concentrations below the detection limit and are therefore not subjected to further analysis in subsequent sampling campaigns, while Pz12 was contaminated with relatively low benzene concentrations in 2021, raising questions about its use as a reference background for the study. Pz18, known as the historically contaminated piezometer, displays a significant decrease in benzene concentration between 2017 and 2020.

This reduction can be attributed to various site operations, including investigations conducted in 2017, which involved drilling, trenching, and soil sampling from selected locations. During these operations, groundwater samples exhibited benzene concentrations well above the VS threshold, while heavily benzene contaminated soil was excavated from identified hotspots (SPAQuE, 2017).

This investigation campaign caused a massive decrease in benzene levels, as its concentration in the groundwater sampling of Pz18 reported in November 2016 was of 45000 µg/L. In fact, the excavation led to benzene volatilization and subsequent re-oxygenation of the aquifer, initiating aerobic biodegradation processes, and resulting in a substantial decrease in benzene contamination. It is important to note that Pz18 is situated along a sidewalk in close proximity to the "Liège Science Park," a frequented area by cyclists, joggers, and pedestrians, as evidenced by the presence of a nearby bench.

Afterwards, on the 14th of October 2020, in situ chemical oxidation (ISCO) was implemented. The immediate effects of ISCO can be observed in the decreased benzene concentration of P301, as this piezometer was located within the injection area (fig. 2.6). The impact on P302 likely occurred at a later stage, as a significant decrease in benzene concentration is evident from the December 2020 sampling campaign onwards.

An exceptional value of benzene concentration was recorded in November 2021, reaching a value of 7500 µg/L. This result stands out due to its significantly elevated level compared to previous measurements. The exact cause of this phenomenon remains unclear, but several hypotheses can be considered. One possibility is the presence of an upward source zone, although it seems unlikely since the contamination did not propagate downgradient towards P302.

Another potential explanation could be the mobilization of trapped contaminants in the bedrock as a result of the push-pull experiment performed in May 2021 or seasonal variations. Fluctuations in groundwater levels, particularly during periods of high water, may have led to the entrainment of residual benzene in the soil. It is worth noting that the trend of benzene concentrations with regards to Pz18 appeared erratic during both spring and autumn (fig. 4.2).
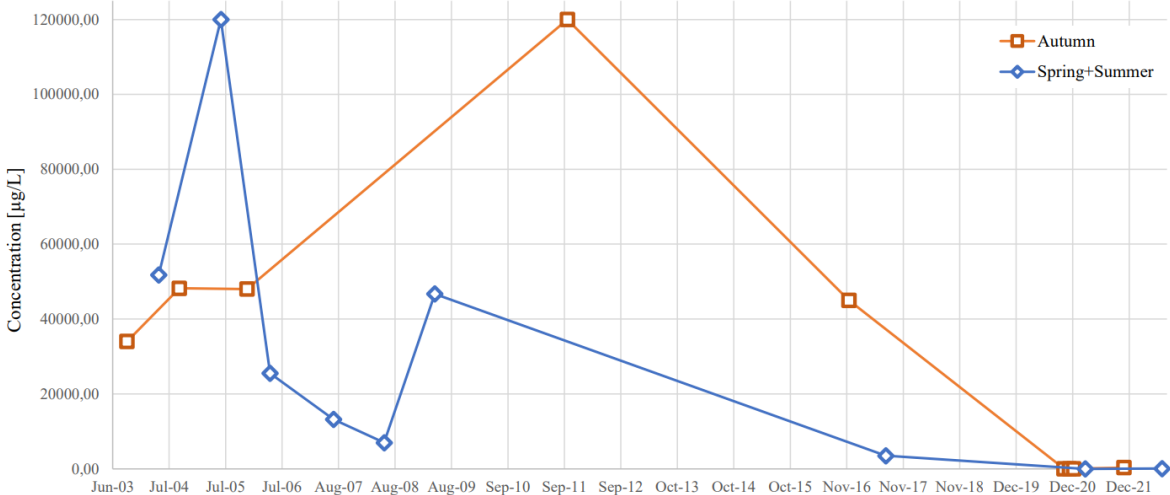
Fig. 4.2. Temporal evolution of benzene concentration in Pz18

Following the excavation operation in 2017 and the subsequent in situ chemical oxidation in 2020, a clear decrease in benzene concentrations can be observed compared to previous years. Furthermore, the graph indicates a general lower concentration during spring compared to autumn, although a peak in spring 2005 exceeded the concentration recorded in the autumn of the same year. The unusually high concentration observed in autumn 2021 could potentially align with this seasonal variation, although the injection of the persulphate agent during the in situ chemical oxidation remediation with the subsequent reactions introduces additional complexities to the interpretation of this phenomenon.

4.2. Previous works on evidencing MNA in Bois Saint-Jean

4.2.1. Overview

This thesis acts as a follow-up to the previous work conducted by Kajsa-Stina Hallberg during the academic year 2020-2021, in her master's thesis titled "Evidencing biodegradation of organic pollutants using push-pull tracer experiments" focused on the same area of investigation in Bois Saint-Jean. Her thesis was drafted several months after the in situ chemical oxidation treatment on October 14, 2020. The primary objective of Hallberg's master's thesis was to evaluate the potential of using reactive push-pull tracer experiments to demonstrate biodegradation of organic chemicals in groundwater.

To gain a deeper understanding about the chemical and biological processes occurring at the site, slug tests were performed. These tests allowed a better comprehension of the hydrodynamics of the site and helped to determine the appropriate dimensioning of the subsequent push-pull experiments, which was performed in the monitoring piezometers P301 and P302.

In a push–pull test, a prepared test solution that contains a non-reactive, conservative tracer and one or more reactive solutes (reactants) is injected ("pushed") into the aquifer through an existing well. During the following initial incubation period, i.e. "resting phase", indigenous microorganisms consume reactants and generate metabolic products.

Thereafter, the groundwater mixture is extracted ("pulled") from the same location. Rates of microbial activities are then determined from an analysis of solute breakthrough curves obtained by measuring concentrations of tracer, reactants and/or metabolic products at the injection/extraction well during the extraction phase of the test (Scroth et al., 2001).

Various tracers in the form of salts were selected: bromide in the form of KBr was chosen as the conservative tracer; sulphate in the form of Na_2SO_4 and nitrate in the form of KNO_3 were used as reactive tracers to investigate their potential as electron acceptors for biodegradation in the site; fluorescein to facilitate visible monitoring directly in the field and observe the evolution of tracer concentrations during the extraction phase.

It is paramount to note that the concentration of nitrate in the site was very low, whereas sulphate was present at high concentrations as a reaction product of the ISCO treatment. Consequently, a higher concentration of sulphate was used to distinguish the injected test solution from the background concentration.

In addition to the push-pull experiments, groundwater samples were collected before the tests to characterize the hydrogeochemical properties of the site. The isotopic ratios of benzene and sulphate in these samples were also measured. During the push-pull tests, the same isotopic ratios were studied in the collected samples, providing valuable information for assessing biodegradation occurring in the proximity of P301 and P302.

The discussion pertaining to the push-pull test is segmented into two distinct paragraphs. Paragraph 4.2.2 will center on the outcomes already delineated in Hallberg's thesis, albeit approached with a fresh perspective and subjected to a thorough re-evaluation from my standpoint. Subsequently, paragraph 5.2.2 will shift its focus to the push-pull test data that were not scrutinized in Hallberg's thesis due to temporal constraints, allowing for an exploration of previously unexamined aspects.

4.2.2. Discussion of interpreted data

The results of the push-pull experiment showed that the recovery of the nitrate tracer was significantly lower than that of bromide in both piezometers. In P301, the recovery of the nitrate tracer was 5.8%, whereas the recovery of bromide stood at 13%. Similarly, in P302, the recovery of nitrate was 18% compared to the recovery of 42% for bromide. These observations suggest the occurrence of biodegradation processes driven by nitrate as an electron acceptor in both piezometers.

Conversely, the recovery of sulphate presented different behaviour. The mass recovery of sulphate was higher compared to the conservative tracer in both P301 and P302, accounting for approximately 50% of the injected concentration, not allowing to draw evident conclusion on MNA with sulphate as electron acceptor through the push-pull experiment.

In addition, by comparing the normalized concentrations of reactive tracers to the normalized concentration of bromide, it is possible to discern the reasons behind the lower tracer concentrations and distinguish the dispersion/dilution mechanisms from biodegradation processes occurring in the groundwater. The BTCs in both P301 and P302 exhibited lower percentages of nitrate recovery compared to bromide throughout the entire pull phase, as the former curve remains below the latter throughout the whole extraction (fig. 4.3). This consistent pattern provides additional evidence of biodegradation processes driven by nitrate as an electron acceptor in both piezometers (Istok, 2013).
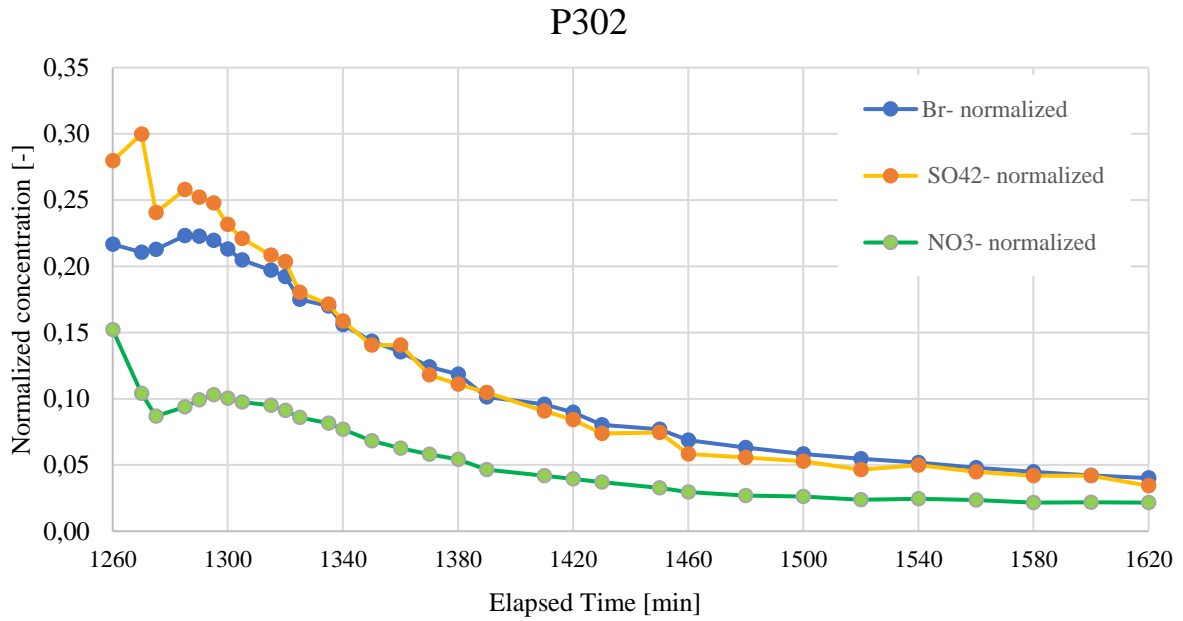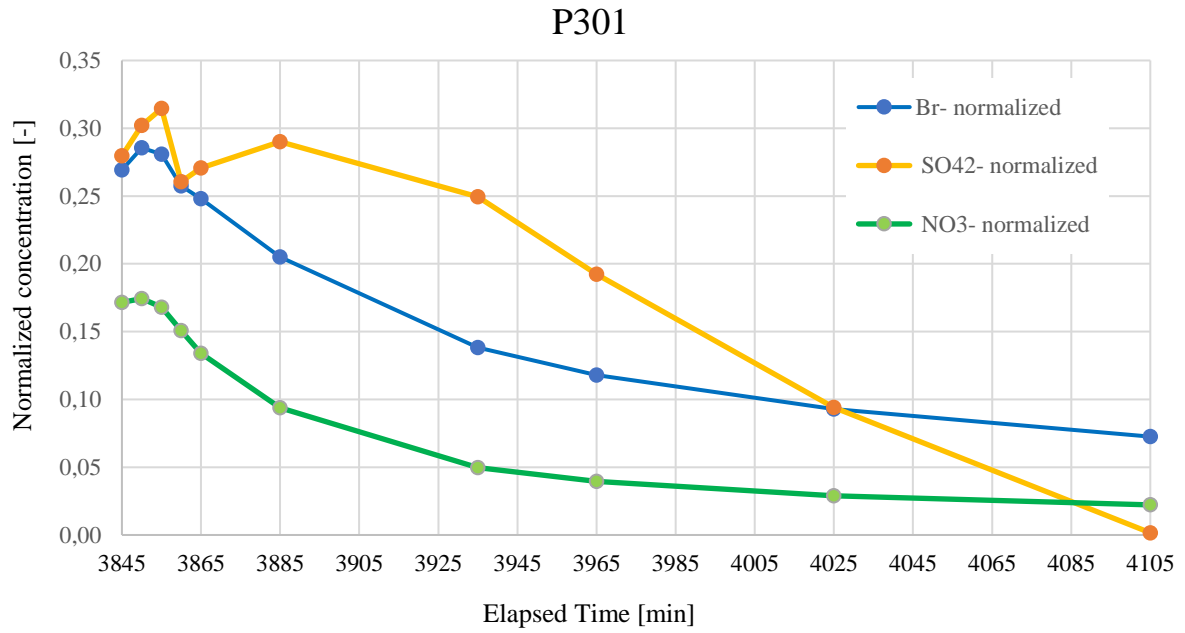
Fig. 4.3. Break through curves of tracers' concentration evolution during push-pull test

The effects of dilution on the NO_3^- breakthrough curve can be removed by plotting dilution-adjusted nitrate concentrations (Istok, 2013):

$$C_{NO3-}^* = \frac{C_{NO3-}}{\left(\frac{C}{C_0}\right)_{Br-}}$$

where C^*_{NO3-} is the dilution-adjusted nitrate concentration in the extracted sample, and $(C/C_0)_{Br-}$ is the relative bromide concentration in the same sample (fig. 4.4).
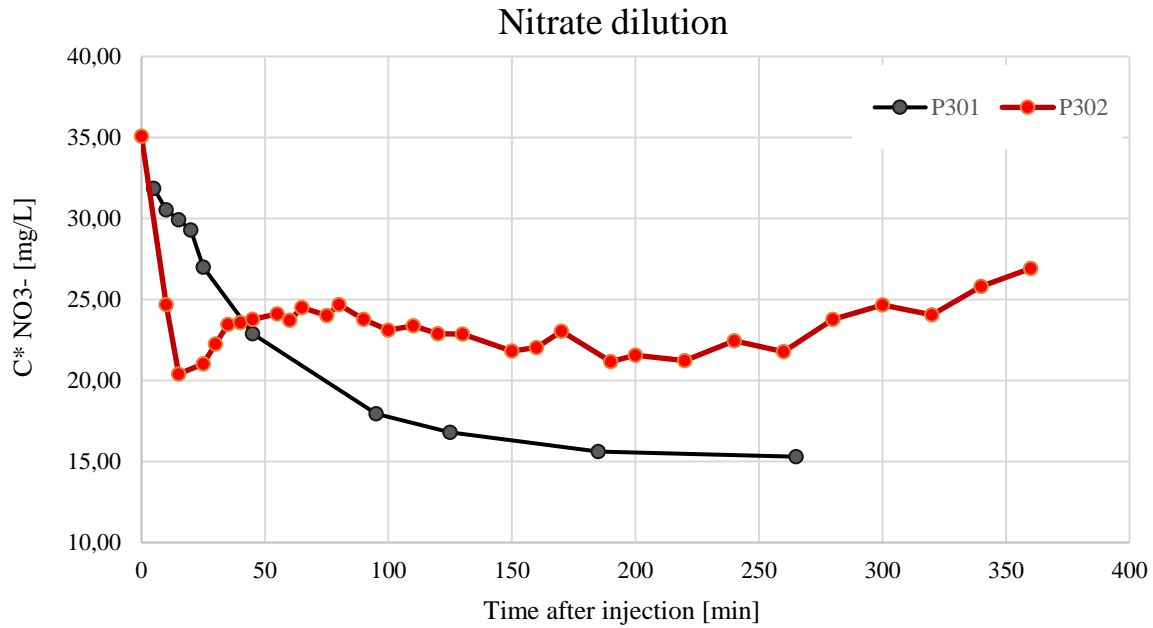
Fig. 4.4. Dilution-adjusted nitrate concentrations with regression line from push-pull test data

The curve for P301 exhibits a clear exponential decline in nitrate concentration over time, potentially hindering active nitrate reduction processes. Conversely, in P302, the initial phase of the experiment shows a considerable decrease in nitrate concentration, whereas the subsequent samples concentrations result in a plateau of the curve. This behaviour may indicate that the potential nitrate reduction in P302 is more limited in space. Such trend could also be affected by the downgradient location of P302 with respect to P301.

With regards sulphate, the recovered concentrations showed a slower decline compared to the other tracers (fig. 4.3). However, drawing precise conclusions is challenging due to several factors that influenced the results. Notably, the high background concentration of sulphate, measuring 884.84 mg/L in P301 and 289.00 mg/L in the downgradient P302, compared to undetectable nitrate concentrations, significantly impacted the interpretations.

Moreover, due to a misreading, there was a considerable difference in the sulphate concentration of the test solution, with 1060 mg/L in P301 and 1720 mg/L in P302, even though conversely the sulphate concentration of P302 is nearly half of P301. Additionally, differences in hydraulic conductivity were observed between P301 (1.7 x 10^{-5} m/s) and P302 (4.8 x 10^{-6} m/s), as determined from the slug test. Lastly, the resting phase for the test solution in P302 was around 21 h, while P301 had a longer resting time of 64 h.

Furthermore, the push-pull test evidenced the occurrence of biodegradation in the vicinity of each piezometer. In fact, lower benzene concentrations compared to the injected ones are recovered during the first part of the pull phase.

However, as the test proceeded, the benzene concentrations eventually returned to the background levels. This phenomenon suggests that biodegradation has taken place near the piezometers, while dispersion has facilitated the mixing of the tracer solution with the background concentration towards the end of the test.

With regards to the isotopic data, the evolution of δ^{13}C-Bz ratios in both piezometers shows an enrichment factor between 2 and 3 ‰ (fig. 4.5), which aligns with the known enrichment factors associated with benzene biodegradation through the reduction of nitrate, as reported in the literature (Meckenstock, 2004).
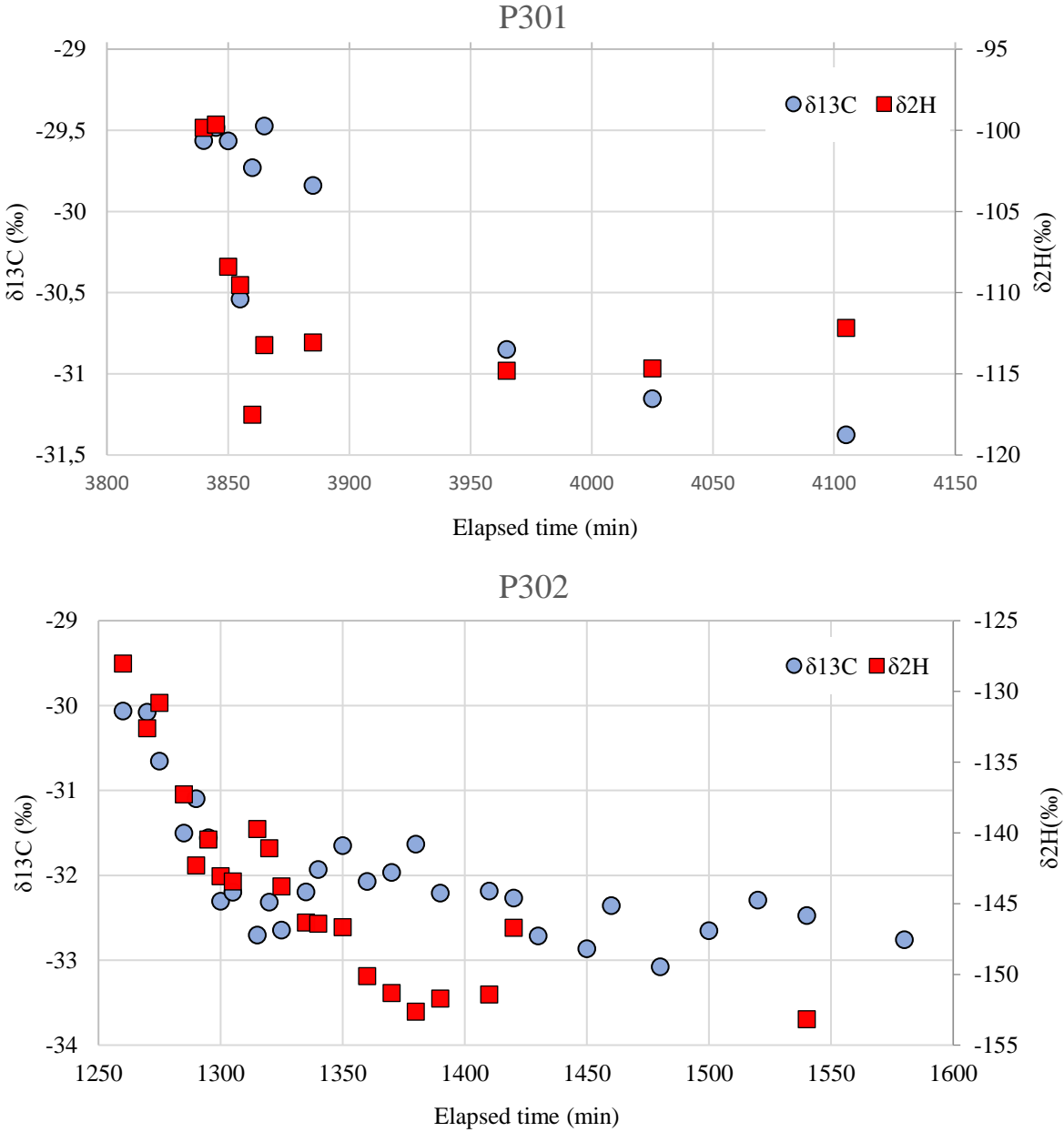
Fig. 4.5. Isotopic fractionation of carbon and hydrogen from benzene during push-pull test

In addition, the δ^2H-Bz evolution allows to further distinguish the different biodegradation biological processes occurring (fig. 4.5). In fact, the isotopic data display a notable deviation from the enrichment factor that would be expected if benzene degradation with sulphate had occurred (Meckenstock, 2004). This discrepancy supports the hypothesis of benzene biodegradation through nitrate reduction.

At this stage of the analysis, a preliminary assessment of the source area reveals potential indications of nitrate reduction, with a more discernible degradation trend observed in P301 compared to P302. Concerning sulphate reduction, instead, the breakthrough curve (BTC) data suggest that despite the significant background sulphate concentrations, there is no ongoing sulphate reduction in the source zone of contamination.

It is crucial to consider that the remarkably high sulphate background concentrations, coupled with the downgradient position of P302 in relation to P301, could be influencing these observations. more comprehensive understanding of the potential for biodegradation through sulphate reduction could have been obtained from the evolution of sulphate isotopes.

Unfortunately, these data were not available for inclusion in the publication of Hallberg's report. However, a detailed discussion of sulphate isotopes and their analysis, along with the isotopic analysis from the groundwater sampled during the February 2023 campaign, is presented in the subsequent section (par. 5.2.2) of this thesis.

5. Hydrogeochemical characterization

5.1. Description of the sampling campaign

5.1.1. Area of investigation

The area under investigation is situated in the south-west region of zone 6 of the ECOREM Bois Saint-Jean zonation, and partially overlaps with the south-west border of zone 13, which corresponds to the surface water Biez-du-Moulin. Given the specific location and the variables of interest, careful consideration was given to select appropriate sampling points. Considering the potential receptors, the availability of piezometers, and the historical pollutant concentrations, a total of five groundwater sampling points and three surface water sampling points were chosen (fig. 5.1).
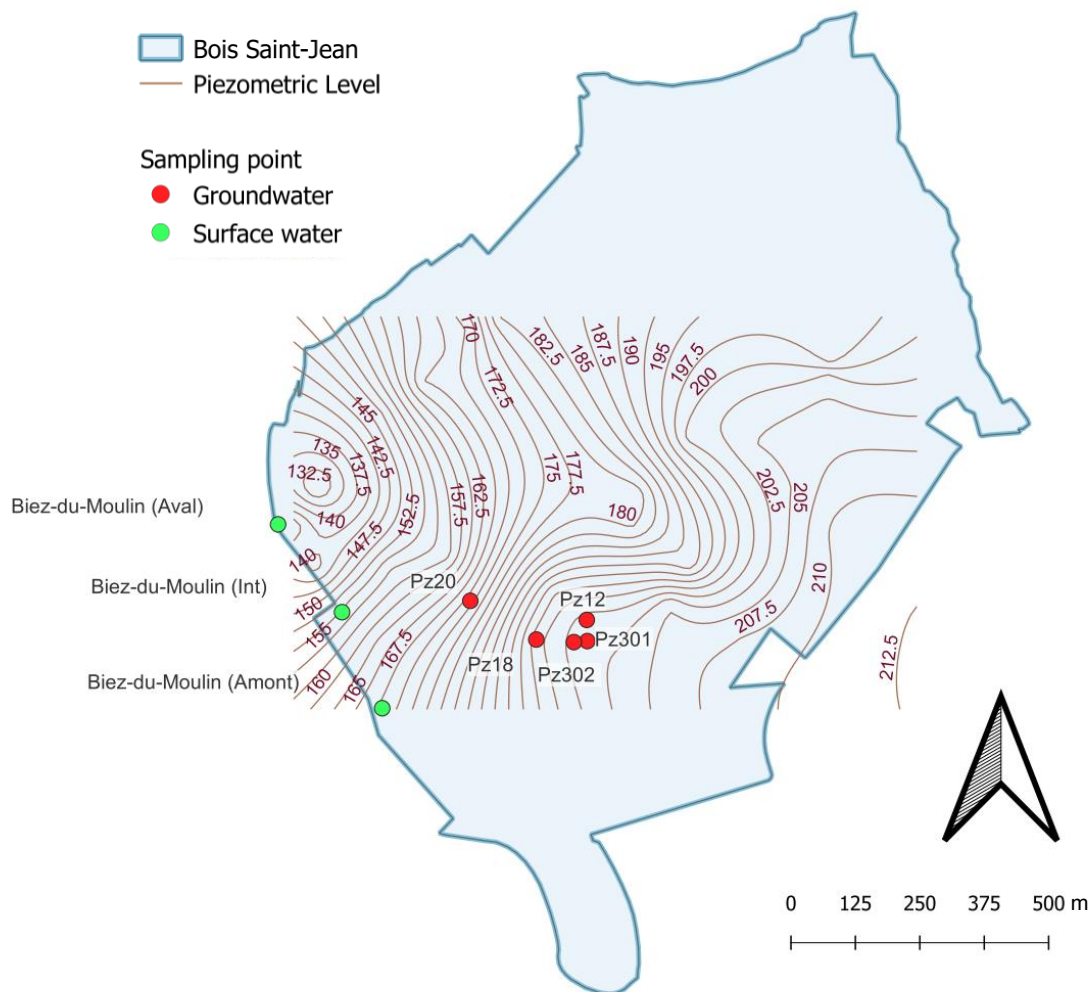
Fig. 5.1. Sampling points and piezometric level of the area of investigation

The objective behind the selection of these sampling points is to establish reference indicators for the normal conditions of the area, data representative of the source area, and data reflecting the downgradient plume area. For the surface water, three locations in Biez-du-Moulin (BdM) were carefully selected to represent the upgradient (Amont), intermediate (Int), and downgradient (Aval) areas of the surface water. This choice aimed to confirm the absence of any discharges into the river and to evaluate potential variations between the upstream and downstream regions. Among the five groundwater sampling points:

- Pz12 served as the upstream piezometer, acting as the reference background

- P301 and P302 represented the source zone

- Pz18 was identified as the hydrologically downgradient piezometer corresponding to the plume and characterized by historical pollution

- Pz20, located downgradient between the source area and the surface water

The piezometric levels within the Bois Saint Jean site exhibit a decreasing trend from around 210 meters at the eastern border to 130 meters at the western border, in the proximity of the downgradient catchment of the Biez-du-Moulin stream. In the source area, the piezometric level remains relatively higher, measuring around 200 meters, while it decreases gradually along the flow path, reaching approximately 195 meters at Pz18 and 170 meters at Pz20. Conversely, the groundwater depth is minimum upgradient at around 8 meters, and maximum downgradient at 13.42 meters, with intermediate values around Pz18 (tab 5.1).

Piezometer	Location	Function	Piezometric Level [m]	Groundwater depth [m]
Pz12	Upgradient	Background reference	201,00	7,86
P301	Source area	ISCO monitoring	201,50	8,19
P302	Source area	ISCO monitoring	200,50	7,90
Pz18	Plume area	Historically polluted	195,00	11,80
Pz20	Downgradient	Plume delimitation	171,00	13,42

Tab. 5.1. Groundwater sampling points characteristics

It is important to highlight that groundwater is predominantly encountered in the fractured shale and sandstones formations within the subsurface. The backfill overlying layer varies in depth, ranging from 1 to 3 meters in P301, P302, and Pz20, while reaching a maximum of 10 meters in Pz18. The underlying layers consist of grey-reddish shale and beige-yellow altered shale, exhibiting heterogeneity within the area. Additionally, the lithological logs of P301 and P302 show an additional layer of black silt with pebbles and wood a few meters thick above the shale formations.

Nearby piezometers were not included in the sampling due to consistently low concentration values below quantification levels in previous campaigns. This allowed for a focused and well-defined investigation area. Additionally, the choice of sampling points was influenced by the availability of functional piezometers, as some others had been damaged or rendered unusable.

A closer examination of the map provides additional insights into the chosen sampling points (fig. 5.2). Notably, a more detailed analysis of the piezometric lines, drawn based on the designated measurement points on the map, raises questions about the appropriateness of designating Pz12 as the reference background site for this study. While initially chosen for this purpose, it is becoming evident that the groundwater flow patterns originating from the source zone around P301 and P301 could potentially extend towards north-east, potentially impacting the theoretical natural conditions at Pz12.

Fig. 5.2. Localization of water samplings and detailed piezometric level of February 2023 sampling campaign

5.1.2. Field sampling and data collection methods

The study was conducted using sensitive data provided by SPAQuE and through the groundwater sampling carried out with SPAQuE's hydrogeologist Dr. Samuel Wildemeersch and PhD student Laura Balzani on February 21, 2023.

The groundwater sampling aimed to gather data on major ions concentrations, BTEX concentrations, biodegradation parameters, isotopes of benzene, nitrate and sulphate, and to perform subsequent microbiological analyses.

To ensure accuracy and representativeness, a sufficient stabilization period was allowed at each sampling location, involving continuous monitoring until steady state conditions were reached. The sampling procedure involved using a portable multi-item water quality meter HANNA HI9829, equipped with an immersed pump PP45, to measure pH, temperature, electrical conductivity, dissolved oxygen, turbidity and redox potential simultaneously and continuously every 5 minutes.

Following SPAQuE's general rules, if after three measurements (15 minutes) the parameters were stable - meaning the difference between the last and the third last values difference is less than 1% - parameters can be considered as stable. Since certain parameters, such as temperature, are extremely variable over time as they are affected by the external conditions, the stabilization is mostly evaluated over pH and electrical conductivity. However, it may happen that a difference below 1% is not reached: in this case the rule of thumb is that the values are taken as such after 10 measurements, i.e. 45 minutes from the start, if no relevant variations are shown.

To monitor groundwater levels and account for potential drawdown effects during pumping, a piezometric probe was used. As a matter of fact, an excessive drawdown caused by the pumping of the water may cause a decrease of the groundwater flow towards the well, leading to significant disturbance of the well conditions and potentially causing the entrainment of solids into the water sample that would not be there under undisturbed conditions (Sevee et al., 2000)

After the stabilization of the parameters, the groundwater samples were taken employing a low-flux technique, with the primary objective of acquiring representative groundwater samples while minimizing disturbances to the subsurface environment. The objective is to pump in a manner that minimizes stress to the system to the extent practical taking into account established site sampling objectives. Typically flow rates on the order of 0.1-0.5 L/min are used, however this is dependent on the site-specific hydrogeology, and they can reach flow rates of 1 L/min. (Puls & Barcelona, 1995). In the case of the groundwater sampling performed on February 21, 2023, the flow rate varied from 0,3 L/min (Pz12) to 0,7 (Pz20 and P301).

Specialized bottles were employed for collecting groundwater samples, tailored for specific parameters. Groundwater samples were collected for major ions analyses using 180 mL plastic vials, carefully filled to the top to minimize air presence.

For benzene isotopes, 40 mL screw cap vials were utilized, treated with 20 µL of mercury dichloride ($HgCl_2$) to prevent contamination. Nitrate isotopes were collected in 60 mL plastic vials, employing 0.2 µm sterile filters during the filling process. Sulphate isotopes were stored in 500 mL plastic vials with the addition of 100 mL of zinc acetate ($Zn(CH_3CO_2)_2$). For microbiological analyses, 5 L plastic vials were meticulously rinsed prior to filling. Throughout the entire sampling procedure, utmost care was taken to position, cap, and fill the bottles properly, minimizing the introduction of air into the samples.

5.2. Results of the hydrochemical analysis

5.2.1. Laboratory analyses and data presentation

The laboratory analyses were performed both by the Department of Geology at the University of Liège and Eurofins Analytico on behalf of SPAQuE. While the characterization will primarily rely on the analyses provided by SPAQuE, the results from the University of Liège serves as a validation of the reliability of the analysis.

The characterization includes in situ measurements, providing real-time information about the groundwater's physicochemical conditions during the sampling campaign in the field. Moreover, BTEX, major ions and geochemical biodegradation indicators concentrations are analysed to understand water's chemical composition and how it varies in different locations.

The results are presented through tables and hydrogeochemical diagrams created with the software *DIAGRAMMES* (Simler, 2012) developed by the Laboratoire d'Hydrogéologie d'Avignon, allowing for a comprehensive understanding of the data and facilitating further investigations into the groundwater system's behaviour.

5.2.2 Sampling location features and in-situ parameters

The following table (tab 5.2) includes the analysis of in situ parameters, including pH, temperature, electrical conductivity, dissolved oxygen, and redox potential along with some location-specific features that contribute to understanding data variability. It is essential to note that measured results may not be fully reliable because air contamination, the temperature and pressure changes during sampling can affect the groundwater chemistry (Sasamoto et al., 2007).

Sample	Type	Elevation [m]	Gw depth [m]	Sampl. depth [m]	pH [-]	T [°C]	EC [µS/cm]	DO [mg/L]	E_h [mV]
Pz12	Groundwater	208,30	9,34	8,50	7,32	8,03	1250,00	0,99	89,00
Pz18	Groundwater	207,90	15,00	13,00	6,07	12,59	1739,00	0,00	84,20
P301	Groundwater	209,94	15,11	14,50	5,96	9,98	664,00	0,00	-136,60
P302	Groundwater	209,71	15,64	13,00	6,20	12,02	737,00	0,00	185,90
Pz20	Groundwater	189,06	24,20	20,00	7,32	10,65	541,00	4,73	74,80
BdM (Amont)	Surface water	≈151,00	/	/	7,33	8,13	781,00	7,62	92,90
BdM (Int)	Surface water	≈167,00	/	/	7,38	8,08	660,00	7,81	93,80
BdM (Aval)	Surface water	≈175,00	/	/	7,57	7,95	598,00	8,15	97,00

Tab. 5.2. Location-specific features and in-situ parameters of February 2023 sampling campaign

The piezometers sampled are situated at an elevation of approximately 208 m, while the surface water is at a lower elevation. Pz20, located between the plume area (Pz18) and the surface water, is instead at an intermediate elevation of 189.06 m.

The depth of water sampled varies across the piezometers, ranging from 8.50 meters in Pz12 to a maximum of 20 m in Pz20, depending on the groundwater depth in each piezometer. Chronologically, the groundwater was sampled in the following order: Pz12, P301, P302, Pz18, and Pz20, thus influencing the variations recorded in the measured temperature (T).

The pH values of the groundwater samples indicate a neutral to slightly basic environment. Pz12 and Pz20 display pH levels close to that of the surface water (average 7.4), indicating minimal influence from contaminants. In contrast, the source area and the plume area show a neutral pH, around 6, most probably influenced by the reaction involved in the ISCO treatment.

The electrical conductivity (EC) of groundwater stands out as relatively high in Pz18 with 1739 µS/cm, lower in the plume area (P301 and P302), and intermediate in Pz12 with 1250 µS/cm. The groundwater conditions are predominantly anoxic, with dissolved oxygen (DO) levels reported to be below 1 mg/L, suggesting that any potential biodegradation is likely to occur under anaerobic conditions, except for Pz20, which is however far from the benzene hotspot.

In terms of redox potential (E_h), it is generally positive in nearly all the piezometers, except for P301, as its negative value deviates from the rest. By measuring the redox potential, we can get an indication of the prevailing redox conditions and infer which electron acceptor is likely to be present and active in the system. However, the redox potential alone is not sufficient to definitively identify the specific electron acceptor present in the area of interest. While certain ranges of redox potential may be associated with specific electron acceptors, there can be overlaps or variations that make the identification challenging (Field, 2002).

P301, with a negative redox potential around -136.60 mV, suggests the likely prevalence of reducing conditions with sulphate or iron as electron acceptors. On the other hand, Pz18 and P302, with a positive redox potential of 185.90 mV, indicates a more oxidizing environment and may be preferential for other electron acceptors such as nitrate or manganese (Beck & Mann, 2010).

Furthermore, the in-situ parameters of temperature in the surface water remain consistently similar at 8°C, whereas the electrical conductivity, dissolved oxygen, and redox potential exhibit similarities but show a slight decrease from upstream to downstream catchments.

5.2.3. BTEX concentration

The table below illustrates the BTEX concentrations (tab. 5.3). As expected, toluene, ethylbenzene, and xylene concentrations are below the detection limit, except for toluene in Pz12, which is regardless very low. Notably, benzene is the only aromatic hydrocarbon of the BTEX group with significant concentrations, and it exceeds the VS threshold set by the 2018 Wallonia Soil Decree exclusively in Pz18.

Aromatic hydrocarbon		VS	Pz12	Pz18	P301	P302	Pz20
Benzène	[µg/L]	10	<0,2	41,00	7,90	0,52	0,21
Toluène	[µg/L]	700	0,54	<0,2	<0,2	<0,2	<0,2
Ethylbenzène	[µg/L]	300	<0,2	<0,2	<0,2	<0,2	<0,2
Xylènes	[µg/L]	500	<0,4	<0,4	<0,4	<0,4	<0,4

Tab. 5.3. BTEX concentration in groundwater samples of February 2023 sampling campaign

When compared to previous investigations (tab 4.1), the benzene concentrations in both Pz18 and P302 are slightly lower than those measured in the last sampling campaign in July 2022, which were respectively 55 µg/L and 0.75 µg/L.

The most striking result is observed in P301, where the benzene concentration is below the regulatory threshold and even lower than Pz18, while in July 2022, it was recorded at 1100 µg/L after reaching a maximum peak of 7500 µg/L in November 2021.

As aforementioned in chapter 4, different hypothesis may be drawn to understand this phenomenon. Seasonal variation, which affects groundwater table flotation, clearly affects the concentration of benzene in the contaminated area. However, the exceptional concentration measured in November 2021 is more likely to be caused by the mobilization of trapped benzene during to the extraction phase of the push-pull experiment performed in May 2021.

Furthermore, the benzene concentration measured in Pz20, though slightly higher than the detection limit, provides valuable insights into the stability of the contamination plume or, eventually, about the downgradient extension limit. This suggest that the contamination does not migrate downgradient, consistently with the absence of BTEX compounds in the surface water, further supporting the hypothesis of no interaction between the plume and Biez-du-Moulin.

5.2.4. Major ions and geochemical biodegradation indicators

The table below (tab 5.4) outlines the concentrations of major anions and cations, complemented by key geochemical indicators of biodegradation, including Fe_{2+} and CH_4, while SO_4^{2-} and NO_3^-, are included in the category of major ions. Along with them, the electrical balance was calculated for each of the water sampling.

Sample	Ca^{2+} mg/L	Mg^{2+} mg/L	Na^+ mg/L	K^+ mg/L	Cl^- mg/L	SO_4^{2-} mg/L	NO_3^- mg/L	HCO_3^- mg/L	Fe^{2+} µg/L	CH_4 µg/L	EB
Pz12	120	56	34	60	19	170	11	580	240	11	0,5%
Pz18	99	63	150	100	54	480	<0,9	500	3700	210	1,3%
P301	24	14	130	5,8	41	230	<0,9	170	8600	370	3,5%
P302	2,3	0,9	180	3,5	30	240	14	150	680	13	2,5%
Pz20	90	22	15	18	5,5	72	1,7	350	440	<2	0,0%
BdM (Amont)	66	17	51	2,0	160	77	6,6	68	/	/	2,6%
BdM (Int)	69	17	49	2,1	150	80	7,4	73	/	/	1,3%
BdM (Aval)	73	18	53	2,8	160	90	8,3	83	/	/	2,5%

Tab. 5.4. Major ions, electrical balance and biodegradation indicators
in water samples of February 2023 sampling campaign

The table provided illustrates that, overall, the three surface water catchments share similarities, displaying minor deviations in the concentrations of major anions without significant implications, as their concentrations slightly increases from upgradient to downgradient.

In contrast, these catchments differ markedly from the groundwater concentrations. Elevated sulphate concentrations are a prominent feature in the sampled groundwater, except for Pz20, together with notable bicarbonate concentrations and relatively low chlorine concentrations. Moreover, no definitive trend can be established for cations in comparison to surface water, except for potassium, which consistently registers at lower concentrations in the latter.

The geochemical indicators of biodegradation offer insights into the dynamic processes occurring within the groundwater samples. In the case of ferrous iron, elevated concentrations are evident, particularly notable in Pz18 and most prominently in P301, where it reaches 8600 µg/L. A similar pattern but with lower order of magnitude emerges with methane concentrations.

In contrast, nitrate concentrations are below detection limits in Pz18 and P301, while being present at very low concentrations in other groundwater samples. Furthermore, sulphate concentrations exhibit remarkable variation, with Pz18 standing out at 480 mg/L, twice the levels observed in P301 and P302.

In addition to the analysis of individual ions, the electrical balance (EB) of the water sampling was computed. This value is based on the principle that in groundwater there are both positively and negatively charged species present as common major solutes. Since the overall groundwater solution should follow the principle of electrical neutrality, the calculation of the electrical helps to ensure the validity and accuracy of the measured concentrations and provides insights into the overall ionic composition of the groundwater. (Deutsh, 1997).

This involves converting the measured concentrations from units like mg/L or ppm to their electrical equivalent units for each major ionic species. The calculation of the electrical balance is then performed by comparing the sum of equivalents attributed to the cations with the sum of equivalents attributed to the anions, computing the following equation:

$$EB = \frac{\sum(cations, meq/L) - \sum(anions, meq/L)}{\sum(cations, meq/L) + \sum(anions, meq/L)} \times 100\%$$

A common rule is that the electrical-balance errors should be less than 5% for groundwater samples (Castro et al., 2018), thus no anoumalous value of EB is contained in the dataset.

5.2.5. First interpretation based on hydrogeochemical diagrams

The hydrogeochemical diagrams presented in this study were generated using *DIAGRAMMES* software, including the Piper, Schöeller-Berkalof, Stiff, and Stabler diagrams.

The Piper diagram (fig. 5.3) contains two triangular charts for depicting the proportions of cations and anions, expressed in meq/L, while, The diamond plot, in which the two data points in the triangles are projected from the intersection of parallel lines, allows for a descriptive chemical composition of groundwater (Appelo & Postma, 2010).

Within this diagram, it is evident that the groundwater samples exhibit varying characteristics. Pz20 and Pz12, representing the least contaminated and least influenced by operational activities, align more closely with the background water type, which predominantly features calcium-bicarbonate composition.

Meanwhile, Pz18, P301, and P302 display a gradual shift from calcium-sulphate waters towards sodium-chloride dominance. In contrast, the surface waters exhibit a distinct pattern of calcium-sulphate composition, setting them apart.

This divergence is further accentuated by the Schöeller-Berkalof diagram (fig. 5.4), in which each sample is represented by a broken line and the concentration of each chemical element is represented by a vertical line in logarithmic scale. The broken line is formed by connecting all the points representing the different chemical elements (Mohareb, et al., 2021).
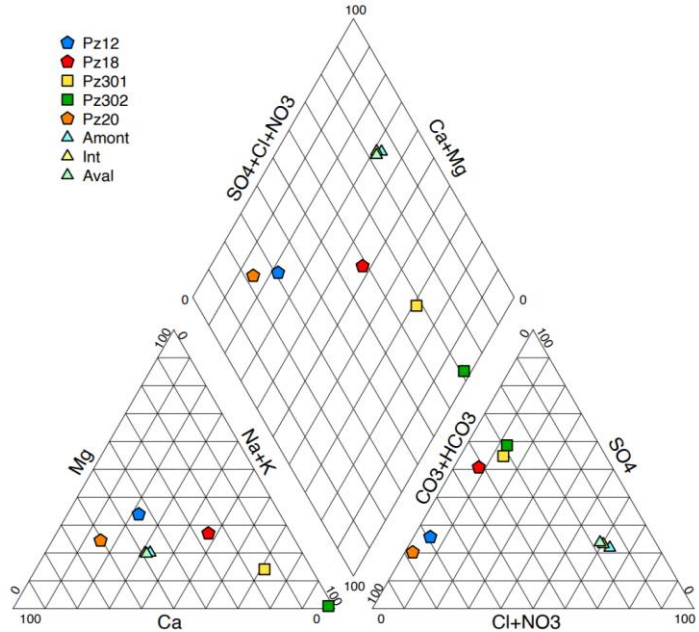
Fig. 5.3. Piper diagram
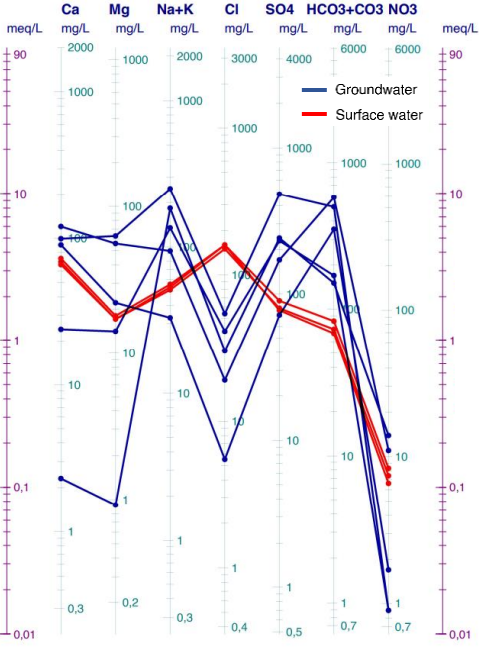
Fig. 5.4. Schöeller-Berkalof diagram

The lines denoting water samples from Biez-du-Moulin overlap, extending beyond all groundwater samples only in terms of chlorine concentrations. Additionally, the Schöeller-Berkalof diagram highlights the overall lower salinity of Biez-du-Moulin waters, a characteristic that aligns with their relatively modest electrical conductivity values compared to the groundwater samples (tab 5.2).

The analysis of the dissolved ions distribution in the groundwater sampled is illustrated with Stiff and Stabler diagram. The Stiff diagram (fig. 5.5) consists of three horizontal axes displaying selected components. On each axis a cation is plotted to the left and anion to the right, again in meq/L (Appelo & Postma, 2010).

This hydrogeochemical diagrams provide further validation of the similarities between Pz12 and Pz20, particularly emphasizing the elevated bicarbonate concentration in the former. These two sampling points stand out by forming shapes that approach hexagonal patterns, while Pz18, P301, and P302 exhibit substantial deviations. Both P301 and P302 share a similar pattern, featuring a higher presence of the sodium-potassium group in the latter, along with a consistently low occurrence of calcium and magnesium.

On the other hand, the polygon representing Pz18 displays a significant area, aligning with its pronounced electrical conductivity. The elongated shape of the Pz18 polygon is attributed to its notably high concentrations of sulphate and sodium+potassium ions.
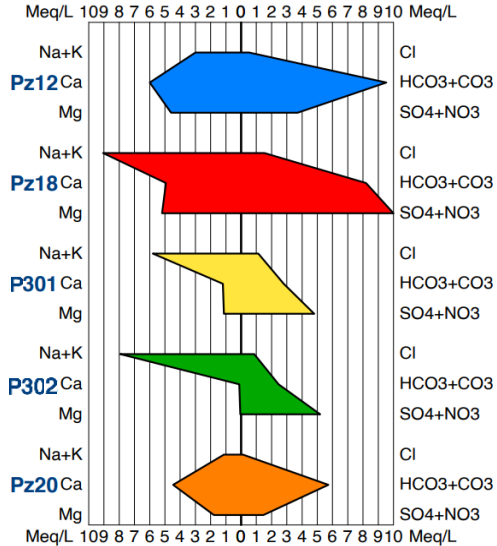
Fig. 5.5. Stiff diagram
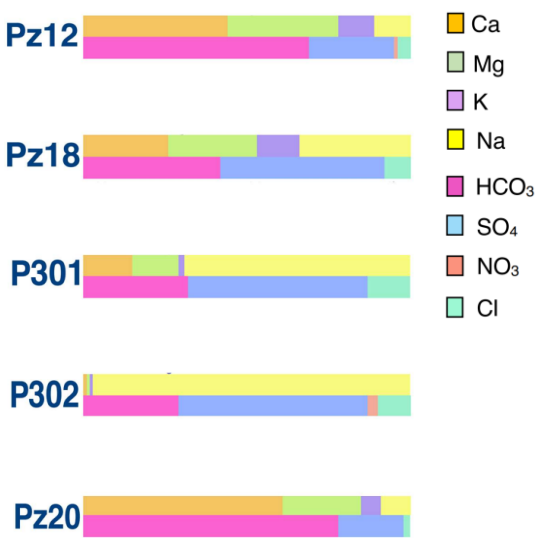
Fig. 5.6. Stabler diagram

A further step in the analysis of the relative concentrations of cations and anions in the groundwater sampled can be performed with the Stabler diagram (fig. 5.6). Stabler classification compares quantities of cations and anions expressed as percentages and separately classifies the anions and cations distribution (Remmani, et al., 2021).

Notably, the prevalence of sodium is evident in the case of P302, where the proportion of sodium ions significantly outweighs that of magnesium, potassium, and calcium ions. Conversely, in Pz20, calcium ions occupy a prominent position, while sodium and potassium ions make up a smaller fraction.

The pronounced presence of sodium in P302 is a direct consequence of the ISCO treatment. This high sodium content arises from the reaction of the persulphate agent utilized in the treatment, as elaborated in section 2.4.2. This is also the reason behind the substantial share of sulphate in P301 and P302, as well as in Pz18. These points exhibit similar anion distributions, which deviate from those observed in Pz12 and Pz20, where bicarbonate ions are more dominant.

Across all groundwater samples, nitrate content is negligibly low and nearly absent, with its presence being so minimal that it remains undetectable on the diagram, with the exceptions of Pz12 and P302, where there is a faint presence of nitrate.

5.2.6. Validation of the data

In order to validate the data outcomes from the University of Liège, a verification process is undertaken involving a direct comparison with analytical findings obtained through assessments performed by SPAQuE. This validation procedure serves as a means of confirming the accuracy, quality, and dependability of the dataset within the studied region.

This validation is visualized through a graph where concentrations of major ions measured by the University of Liège are plotted on the x-axis, while concentrations measured by SPAQuE are plotted on the y-axis (fig. 5.7). Points that align along the red-dashed 1:1 line signify a perfect match between the two datasets.

Upon examination of the graph, it becomes evident that there is a substantial overall alignment of the data points with the 1:1 line, indicating a high degree of consistency. Notably, the concentrations from both sources closely track each other, emphasizing the robustness of the data obtained through SPAQuE's analysis.

However, a more distinct divergence is observed in the case of nitrate measurements. It is important to underscore that a direct comparison of nitrate concentrations may not be entirely reliable, given that the University of Liège has a lower detection limit compared to SPAQuE (0.9 mg/L). Consequently, some concentrations that are measurable by the University of Liège are not detected by SPAQuE's measurements.
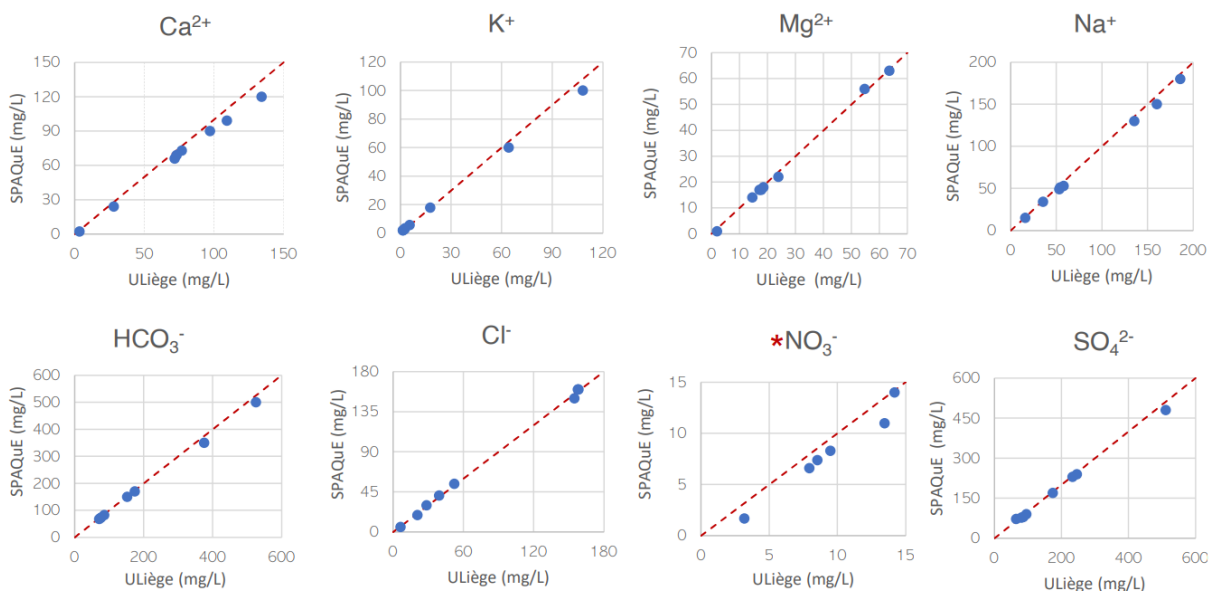

Fig. 5.7. Comparison between the data measured by University of Liège and SPAQuE in the sampling campaign of February 2023

5.3. Isotopic data analyses

5.3.1. Laboratory analysis

The isotopic data extracted from groundwater samples acquired during the sampling campaign on 21st February 2023 were supplied by Dr. Kay Knöller from the Helmholtz Centre for Environmental Research (UFZ). These data include the following isotopic stable isotope ratios:

- $\delta^{13}C$-DIC V-CDT, to assess benzene degradation processes

- $\delta^{34}S$-SO_4^{2-} V-CDT and $\delta^{18}O$-SO_4^{2-} V-SMOW, to assess potential sulphate reduction

- $\delta^{15}N$-NO_3^- V-AIR and $\delta^{18}O$-NO_3^- V-SMOW to assess potential nitrate reduction

These isotopic measurements, conducted using the Compound-Specific Isotope Analysis (CSIA) approach, can be instrumental in evaluating the extent of benzene biodegradation and whether nitrate or sulphate reduction pathways are prevalent in the different piezometers, aiding in drawing comparisons across the various sampling points.

The interpretation of the isotopic data analyses will also encompass the sulphate isotopic data derived from the push-pull test conducted in May 2021 as part of Hallberg's master's thesis.

Also these data were provided by Dr. Kay Knöller from the Helmholtz Centre for Environmental Research (UFZ). The sulphate isotopic data were not previously interpreted in the earlier study due to time constraints and are thus brought into consideration within the current analysis.

5.3.2. Sulphate isotopic data from the push-pull test

This paragraph explores the unaddressed sulphate isotope evolution data, with the goal of further investigating if the conditions of the groundwater in the source area are favourable for the benzene degradation by sulphate reduction.

The exploration of isotopic signature evolution during push-pull tests has proven valuable in proving sulphate reduction processes. However, it's important to recognize that previous push-pull experiments have typically involved lower tracer concentrations in the background, compared to the injected tracer concentration (Burbery et al, 2004; Kleikemper J. et al., 2002; Schroth et al., 2001).

In the present study, a distinct situation arises due to the significant elevated background sulphate concentration in the area of investigation resulting from the ISCO treatment. For this reason, the defined method found in the literature is modified taking into account the relevant differences.

The model proposed relies on the strong underlying assumption that the variation of the isotopic signature of the injected sulphate tracer $\Delta\delta^{34}S_{inj}$ mirrors that of the naturally occurring background sulphate $\Delta\delta^{34}S_{bg}$, i.e., $\Delta\delta^{34}S_{inj} = \Delta\delta^{34}S_{bg} = \Delta\delta^{34}S$.

Under this important premise, the following equation that accommodates the specific conditions of this study can be considered:

$$\delta^{34}S = f \times \left(\delta^{34}S_{inj} - \Delta\delta^{34}S\right) + (1 - f) \times \left(\delta^{34}S_{bg} - \Delta\delta^{34}S\right)$$

The equation can be rearranged to isolate the term relative to the variation of the stable sulphur isotope ratio $\Delta\delta^{34}S$ of sulphate, resulting in:

$$\Delta\delta^{34}S = (1 - f) \times \delta^{34}S_{bg} + f \times \delta^{34}S_{inj} - \delta^{34}S$$

where f is the dilution factor, calculated as the ratio between the measured concentration of bromide at each sample and the injected ones, $\delta^{34}S_{bg}$ is the background signature of the stable sulphur isotope ratio of sulphate, $\delta^{34}S_{inj}$ is the stable sulphur isotope ratio of sulphate in the test solution injected, $\delta^{34}S$ is the stable sulphur isotope ratio of sulphate measured at each sample.

Consequently, a positive shift in $\Delta\delta^{34}S$ would indicate the potential presence of sulphate reduction processes within the groundwater system. The same approach is used for the computation of the variation of stable oxygen isotope ratio $\Delta\delta^{18}O$ of sulphate. The results deriving from the application of the equation are displayed in a graph illustrating the isotopes temporal evolution during the extraction phase of the push-pull experiment (fig. 5.8).

Built upon the robust assumption aforementioned, the graphical representation distinctly reveals that P302 experiences a minor variation in $\delta^{34}S$-SO_4^{2-}, dropping below zero in the initial phase of extraction and maintaining proximity thereafter. In contrast, P301 distinctly demonstrates an upward trajectory in $\delta^{34}S$-SO_4^{2-} variation, indicating a potential pathway of degradation through sulphate reduction. Additionally, a noteworthy observation from the graph is the correspondence between the variations in $\delta^{18}O$-SO_4^{2-} and $\delta^{34}S$-SO_4^{2-}, reinforcing the conclusions which could be drawn from the plot.
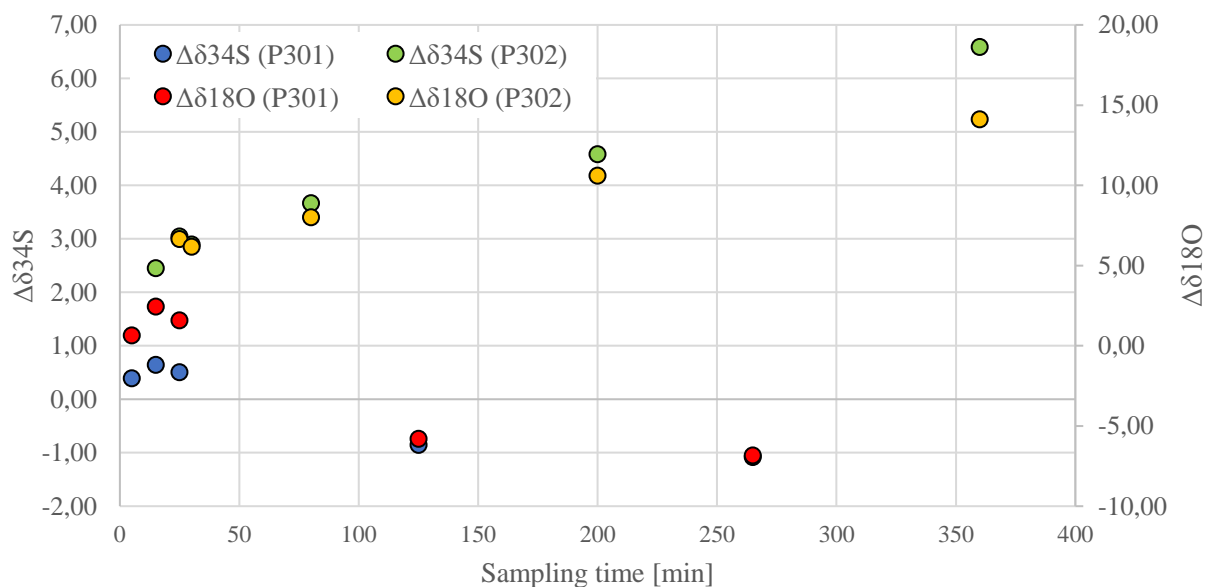
Fig. 5.8. Variation of stable sulphur and oxygen isotope ratio of sulphate during push-pull test, corrected with the bromide dilution factor

5.3.3. Carbon isotopes

The following table shows the results of stable carbon isotope ratio of dissolved inorganic carbon δ^{13}C-DIC (tab 5.5).

	Pz12	Pz18	P301	P302	Pz20
δ^{13}C-DIC (‰)	-16,8	-11,6	-9,7	-13,2	-15,5

Tab. 5.5. Stable carbon isotope ratio (δ^{13}C) of dissolved inorganic carbon (DIC) measured in the groundwater samples of February 2023 sampling campaign

Under normal circumstances, it is expected that δ^{13}C-DIC in groundwater would display depletion due to ongoing biodegradation (Kanwartej et al., 2022). The oxidation of hydrocarbons in groundwater directly generates CO_2, which dissolves into the water, forming mainly HCO_3^- and H_2CO_3. As a result, the DIC of the watershould increase in proportion to the hydrocarbon mineralization (Seagren & Becker, 2002). Consequently, microbial respiration produces isotopically light DIC and will tend to lower the δ^{13}C–DIC along a groundwater flow path in the absence of significant inputs of DIC from other sources with a different isotope signature (Smith et al., 2011).

However, the condition of the site of investigation cannot be considered as normal, as they are heavily affected by former remediation works. In particular, fluctuations in DIC can be induced by the same factors responsible for pH shifts (Quay et al., 1986).

In area of investigation, the release of CO_2 and H^+ during the ISCO remediation technique (refer to par. 2.4.2) significantly impacts pH, evident by lower pH values in the injection zone (P301 and P302) and downstream in Pz18, compared to the other groundwater samples. This could potentially explain why, despite Pz18, P301, and P302 being contaminated piezometers, they exhibit enriched δ^{13}C-DIC compared to Pz12 and Pz20, which defies the conventional expectations.

Furthermore, the ISCO process might have also influenced the total alkalinity in the source area, leading to notably lower values in P301 and P302. This could result in CO_2 degassing from groundwater, possibly affecting δ^{13}C-DIC values.

Additionally, the formation of ^{13}C-rich HCO_3^- during methanogenesis can lead to elevated DIC concentrations with relatively high δ^{13}C values (Chatterjee et al., 2011). Notably, methane levels are particularly elevated in Pz18 and P301 compared to other piezometers, offering an alternative explanation for the unexpected results. Nevertheless, these assumptions remain theoretical and provide only partial insight into the peculiar behavior of these isotope values.

5.3.4. Nitrate isotopes

The following table shows the results of stable nitrogen and oxygen isotopes ratio of nitrate δ^{15}N-NO$_3^-$ and δ^{18}O-NO$_3^-$ (tab 5.6). Isotope analysis requires a certain minimum concentration to yield a detectable signal, and since nitrate concentrations are extremely low, this can lead to weak or absent isotopic signals. Specifically, low to very low signals were observed in Pz20, Pz18, and no signal was obtained in P301, where the nitrate concentrations were below detection level, resulting in data not available.

	Pz12	Pz18	P301	P302	Pz20
δ^{15}N-NO$_3^-$ (‰)	11,4	39,3		13,1	4,1
δ^{18}O-NO$_3^-$ (‰)	3,9	43,2		8,8	8,3
comment		very low signal	no signal		low signal

Tab. 5.6. Stable nitrogen and oxygen isotope ratio (δ^{15}N and δ^{18}O) of nitrate (NO$_3^-$) measured in the groundwater samples of February 2023 sampling campaign

Positive isotopic shifts of both species strongly indicate that nitrate is consumed by the anaerobic bacterial denitrification processes (Müller, et al., 2021). Denitrification normally leads to an equal fractionation of δ^{18}O and δ^{15}N which means that isotopes change in parallel (Granger et al., 2008).

Unusual negative shifts, especially for oxygen isotopes, are an indicator for reverse reactions of intermediates (for example nitrite), which can influence the isotopic signal of the residual nitrate pool (Casciotti et al., 2011).

Pz18 stands out with clear indications of nitrate reduction, as it exhibits substantial enrichment in both $\delta^{15}N\text{-}NO_3^-$ and $\delta^{18}O\text{-}NO_3^-$ isotopic values, distinguishing it from the other samples. In the case of P302, a modest positive isotopic shift suggests potential nitrate reduction, although to a lesser extent. By considering Pz20 as representative of uncontaminated background conditions, the isotopic signature in Pz12 suggests an enrichment in $\delta^{15}N\text{-}NO_3^-$ coupled with a depletion in $\delta^{18}O\text{-}NO_3^-$, possibly implying the occurrence of reverse reactions. It's important to highlight that while Pz12 has benzene concentrations below the detection limit, Pz20 records benzene levels just above this limit at 0.21 µg/L.

5.3.5. Sulphate isotopes

The results obtained from the sulphate isotopes analysis can be complemented by the findings from the March 2021 sampling campaign outlined in Hallberg's master's thesis. By merging information from these two separate sampling periods, it is possible to potentially identify patterns and trends over time, contributing to a deeper understanding of the sulphate reduction within the site of investigation. The evolution of these data is illustrated through a dual isotope plot, where the variations in $\delta^{18}O\text{-}SO_4^{2-}$ and $\delta^{34}S\text{-}SO_4^{2-}$ ratios are showed (fig. 5.9).

The simultaneous occurrence of an enrichment of the heavy sulphur isotope ^{34}S in the residual dissolved sulphate in concert with the apparent oxygen isotope equilibration between the residual sulphate pool and the ambient water is typical for bacterial sulphate reduction (Feisthauer, et al., 2012).

An enrichment of $\delta^{34}S\text{-}SO_4^{2-}$ with slight increase of $\delta^{18}O\text{-}SO_4^{2-}$ is detected in Pz18, hindering potential degradation by sulphate reduction bacteria, whereas the positive shift in Pz12 is coupled with the doubling of the oxygen isotope.

Although both sulphur and oxygen isotopes are partitioned during each intracellular step, their relative behaviour in the natural environment is not fully understood (Antler, et al., 2013). In fact, the sulphur isotope composition of sulphate ($\delta^{34}S\text{-}SO_4^{2-}$) typically increases monotonically as bacterial sulphate reduction progresses (Rees, 1973).
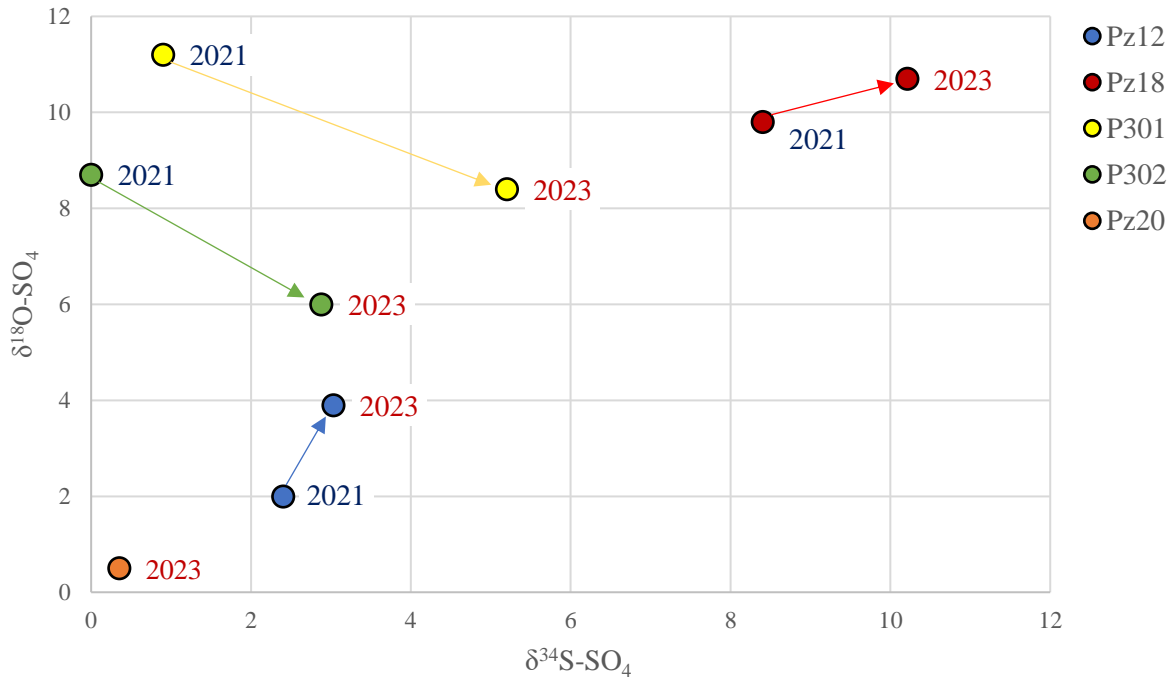
Fig. 5.9 Dual isotope ratio of $\delta^{34}S$ and $\delta^{18}O$ of sulphate (SO_4^{2-}) evolution

On the other hand, the $\delta^{18}O$-SO_4^{2-} has shown variable behaviour during bacterial sulphate reduction in natural environments. In some cases, the $\delta^{18}O$-SO_4^{2-} exhibits a linear relationship with $\delta^{34}S$-SO_4^{2-}, also suggesting a distillation of the light isotope from the reactant sulphate. In most measurements of $\delta^{18}O$-SO_4^{2-} during bacterial sulphate reduction, however, the $\delta^{18}O$-SO_4^{2-} increases initially until it reaches a constant value and does not increase further, while the $\delta^{34}S$-SO_4^{2-} may continue to increase (Antler, et al., 2013).

In fact, in case of an equilibration-dominated behaviour, the assumption of a positive linear relationship between $\delta^{18}O$-SO_4^{2-} and $\delta^{34}S$-SO_4^{2-} is valid only if $\delta^{18}O_{EQ}$ is higher than $\delta^{18}O$-SO_4^{2-} initial (Knöller et al., 2006). A lower $\delta^{18}O_{EQ}$ would result in a negative slope of the $\delta^{18}O$-$\delta^{34}S$ relationship, which could potentially explain the behaviour of P301 and P302.

Interpreting the relative evolution of the $\delta^{18}O$-SO_4^{2-} and the $\delta^{34}S$-SO_4^{2-} during bacterial sulphate reduction in natural environments, and what this relative evolution indicates about the enzymatic steps during sulphate reduction, remains confounding (Antler, et al., 2013).

For this reason, another approach that could be used involved the comparison between $\delta^{34}S$-SO_4^{2-} and sulphate concentrations evolution, in terms of ratio between the concentration measured in 2023 with the concentration measured in 2021.

Increasing $\delta^{34}S$-SO_4^{2-} values in concert with decreasing sulphate concentrations provide further evidence for the occurrence of sulphate reduction (Müller et al., 2021).

The ratio of sulphate concentrations was normalized to chloride concentrations to account for any dilution/dispersion effects occurred between the two sampling campaigns on the increase in sulphate concentration:

$$normalized\ sulphate\ concentration\ ratio = \frac{[SO_4^{2-}]_{2023} / [SO_4^{2-}]_{2021}}{[Cl^-]_{2023} / [Cl^-]_{2021}}$$

It's important to note that the comparison can be performed for all the groundwater samples except for Pz20, which was not part of the sampling campaign in March 2021. For this reason, its value is not displayed in the following graph (fig. 5.10).
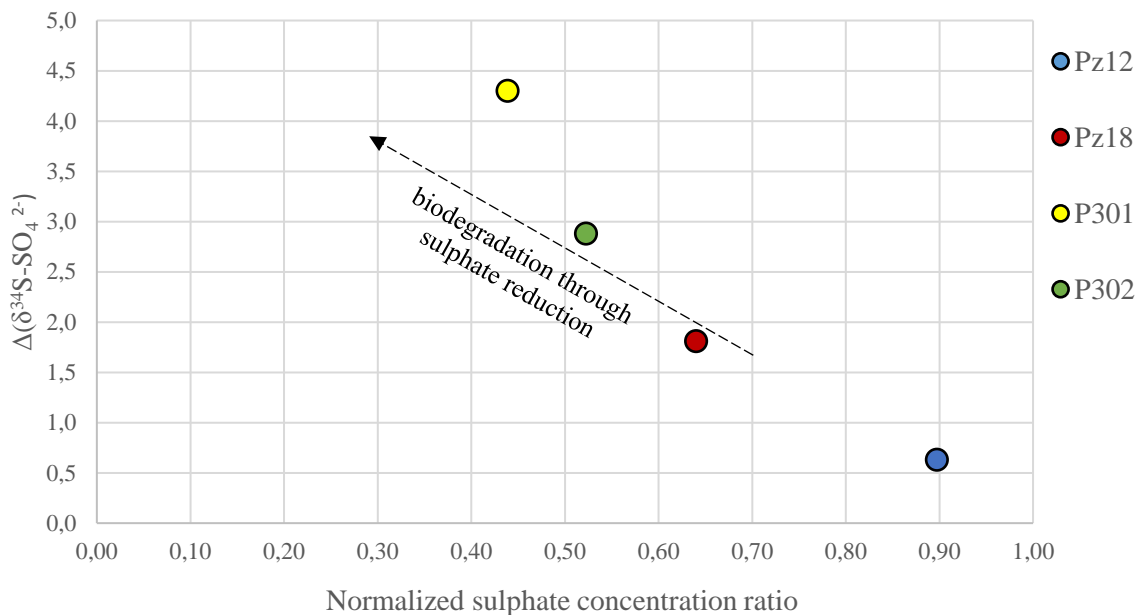
Fig. 5.10. Comparison between $\delta^{34}S$-SO_4^{2-} and sulphate concentrations evolution

In the case of Pz12, the enrichment in sulphur isotopes is characterized by a relatively low variation, mirroring the modest changes in sulphate concentration. This observation suggests that sulphate reduction processes might not be prominent in this piezometer.

Conversely, a substantial positive shift in sulphur isotopes, coupled with a significant reduction in sulphate concentration, is evident in P301. This intriguing trend might point towards the occurrence of sulphate reduction processes.

Similar hypothesis can be drawn for P302 and Pz18, where even though the extent of sulphate concentration reduction is less pronounced, the consistent positive shifts in sulphur isotopes warrant further investigation into the potential sulphate reduction activities in these locations.

5.4. Microbiological analyses

5.4.1. Microbial laboratory filtration

Microbial analyses were conducted using the 16S-rRNA sequencing technique on samples collected during the sampling campaign performed on February 21, 2023. In the field, 5 L containers were filled for each sampling, minimizing the introduction of air. Subsequently, three days after collection, water filtration was carried out with the PhD student Laura Balzani at the Institut Scientifique de Service Public (ISSeP) Laboratory. The filtration was accomplished using an Ez-Stream^{TM} vacuum filtration pump, directing the sampled water through 0.2 μm filters within Millipore Sigma^{TM} Microfil funnels.

Various filtration rates were observed during this process. After four hours of filtration, the process was interrupted due to filter clogging, strongly limiting the water flow. As a result, 3.25 L of water from Pz12 and Pz20, the least polluted samples, were filtered. In the case of P301, instead, 1.40 L of water underwent filtration, while for Pz18 and P302, only 1.25 L were filtered, due to a very limited flow rate across the filter. Notably, P302 required the use of two distinct filters due to the exceptionally low flow rate of the first.

Afterwards, bacteria trapped in the filters were dislodged using a sterilized stick and transferred to vials containing 2 mL of DNA stabilizer. The vials were then stored in the freezer, before being analysed by the Department of Food Sciences and Microbiology of the University of Liège, which performed the 16S-rRNA targeted sequencing. The resulting analysis outcomes were then provided by Dr. Bernard Taminiau, who played a significant role in guiding the consultation and interpretation of the findings.

5.4.2. Principal Coordinate Analysis

To gain first insights into the variations in microbial populations across different samplings, Principal Coordinate Analysis (PCoA) can be employed as a powerful tool for analysing the microbial community structure.

It is essential to note that the utilization of Principal Coordinates Analysis (PCoA) with only five samples and a single campaign yields a broad descriptive perspective. In fact, statistical analysis generally requires a larger sample size to draw meaningful conclusions. With such a limited dataset, the PCoA visualization might offer a basic overview of patterns but may lack the statistical robustness necessary to uncover subtle relationships or trends.

The PCoA method is implemented in this study due to its more satisfactory handling of missing data compared to PCA (Rohlf, 1972). This distinction arises from the fact that PCoA begins with a dissimilarity or similarity matrix, unlike PCA which originates from the initial data matrix (Mohammadi & Prasanna, 2003).

The inherent uncertainty arising from the small sample size makes it however difficult to draw definitive conclusions. Additionally, the single time point assessment provides a snapshot view and doesn't capture potential temporal variations that might occur over time. For this reason, the obtained insights should be seen as preliminary and warrant further validation and expansion through other sampling campaigns to provide a more comprehensive understanding of the system dynamics.

The PCoA can be illustrated with Bray-Curtis dissimilarity matrices of OTUs at 97% cutoff created using RStudio (fig. 5.11). This matrix allows to reduce the high-dimensional microbial community data into two (or more) dimensions, allowing for easier visualization while retaining the dissimilarity structure between samples.

In the specific case of this study, the axis PCoA-1 and PCoA-2 represent the most significant sources of variation in the dataset. The arrangement of samples along the axes of the PCoA plot provides valuable insights into the microbial community structure and its relationship with contamination levels.
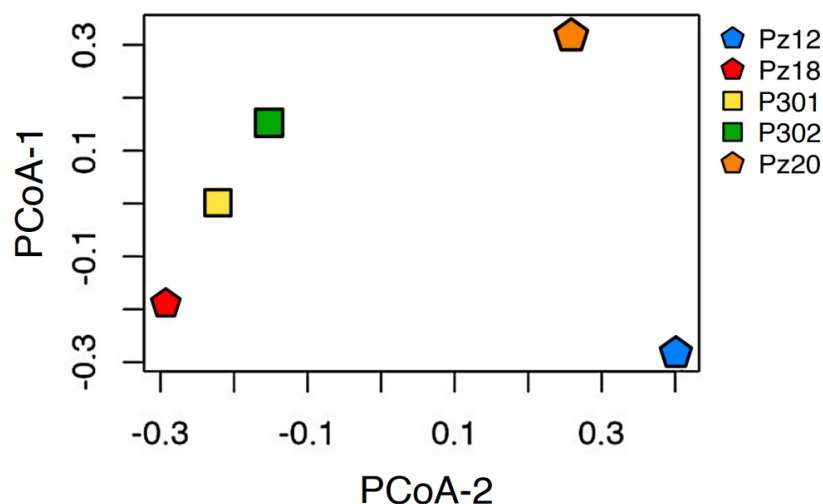

Fig. 5.11. Principal Coordinate Analyses Bray-Curtis dissimilarity matrix

Along the x-axis (PCoA-1), samples are ordered from left to right, reflecting a likely gradient of contamination. On the leftmost side, samples exhibit higher contamination, with Pz18 occupying the lowest position along this axis, followed by P301, and then P302 at the higher

end. The right side of the graph is instead occupied by Pz12 and Pz20, the least contaminated piezometers, with a clear distinction on the PCoA-2 axis between the two piezometers, illustrating the different conditions in which they are.

In fact, the microbial community in these two samples may differ due to geographical and geochemical conditions, as Pz12 is upgradient while Pz20 downgradient, but it may also differ due to potential contamination that influences the diversity of the microbes present in the vicinity of the sampling locations.

5.4.3. Microbial community composition

Evaluating the microbial community composition at the phylum level through a relative abundance graph provides insight into the predominant microbial taxa present in the sampled environment. This graph offers a visual representation of the proportional distribution of various phyla within the microbial community. However, relying solely on a single sampling campaign for this type of analysis has its limitations. Microbial communities can exhibit temporal variability due to factors like environmental conditions (e.g. redox potential, temperature, seasonal and water table variations) and nutrient availability. Therefore, a single time point may not capture the complete range of microbial dynamics, potentially leading to an incomplete understanding of the community structure.

Taxonomy identification is performed through an iterative process using the SILVA database, which allows matching the generated 16S-rRNA sequences to known microbial taxa, aiding in accurate taxonomic assignment. Nonetheless, it's important to note that through 16S-rRNA sequencing, only a fraction of the filtered microbial genome is amplified and analysed. This can result in a skewed representation of the microbial community, as certain taxa may be overrepresented while others remain undetected. This limitation underscores the need for caution in interpreting the relative abundance results, as they reflect the amplified portion of the community rather than the entirety.

Despite this, the analysis of microbial community composition serves as a valuable tool for discerning the presence of key microbial communities associated with benzene degradation in groundwater and understanding their structural variability across different sampling points.

Through taxonomy classification data, it was revealed that dominant phyla such as Proteobacteria, Patescibacteria, Dependentiae, Desulfobacteria, and Firmicutes collectively constitute over half of the total microbial composition within the piezometers (fig. 5.12). Phylum "Bacteria_ph" clusters sequences which could not be attributed to a known phylum.
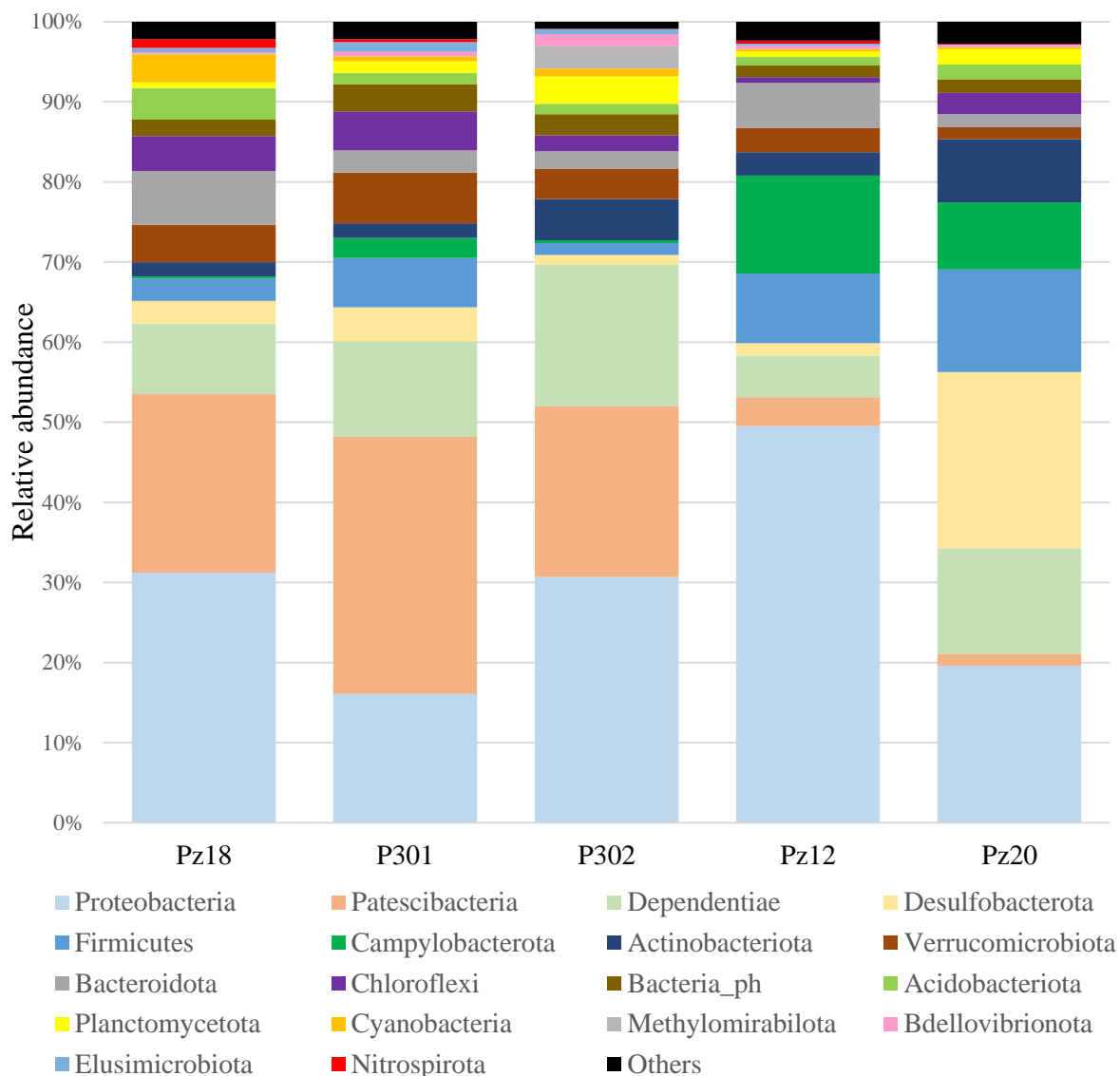
Fig. 5.12. Relative abundance of bacteria taxa at the phylum level

However, their distribution displays notable differences among the five groundwater samples. This distinction becomes more pronounced when examining the microbial community at the family and genus levels, allowing a finer resolution of the variations in microbial composition among the different piezometers.

In the group of Proteobacteria identified, a significant number of bacteria unrelated to benzene degradation were detected, included *Holosporaceae* (Fahy et al., 2006) and *Legionella*, where the latter is a common, yet poorly understood waterborne pathogen (McBurnett et al., 2018).

Nevertheless bacteria belonging to Proteobacteria of relevance in the context of this study were also found. Notably, an abundant presence of *Rhodocyclaceae* was observed in Pz12, which together with *Azoarcus* - also present in Pz12 but with a relatively low abundance - has been documented to be involved in nitrate-dependent benzene degradation (Keller et al., 2018).

In Pz18 it was instead identified a large presence of *Methylocystis*, methanotrophs involved in the removal of methane produced during benzene degradation (Ryu & Cho, 2012).

Most of the Patescibacteria found in the samplings belong to the class of Parcubateria, which have not yet been cultivated, resulting in limited knowledge in the literature. Nonetheless, a genus belonging to Patescibacteria is *Saccharimonadales*, bacteria involved in the degradation of aromatic compounds (Yang, et al., 2023), is among the predominant genera detected in Pz18, P301 and P302. Moreover, *Kaiserbacteria,* nitrite reducer bacteria*,* were intensively present in Pz18, P301 and P302. The action of these organisms has been documented to be very important in environments where the nitrogen is often in limited concentrations (Toumi, et al., 2021).

Dependentiae, whose relative abundance is significative and varies among the different piezometers, stands as one of many phyla within the not-yet cultivated bacteria, resulting in a poor documented phylum (Weisse et al., 2022).

Omnitrophiceae, denitrifying bacteria (Mengyuan, et al., 2023) belonging to *Verrucomicrobiota*, are present in Pz18, P301 and P302, with Pz18 containing also *Nitrospira*, involved in the nitrogen metabolism.

On the contrary, bacteria involved in the sulphur metabolism were notably found in Pz12 and Pz20. Specifically, sulphate-reducing bacterium of the genus *Desulfatirhabdium* belonging to the *Desulfobacterota* can be largely detected in Pz20, whereas *Pseudomonas* species, which perform sulphate reduction more intensively under strictly anaerobic conditions than under aerobic conditions (Kliushnikova et al., 1992), is less abundant but still detected in Pz12. Facultatively anaerobic, chemolithoautotrophic, sulfur-oxidizing bacteria belonging to the genera *Sulfuricurvum* and *Sulfurimonas* and thus to the Campylobacteria phylum, are instead present in both Pz12 and Pz20. Although these bacteria are detected also in the other samples, their quantity is relatively scarce.

5.4.4. Assessment of degradation pathways

To identify the current or potential degradation pathways operating within the groundwater samples, a robust tool known as KEGG Orthology (KO) system, was implemented. KO system is a pathway-based classification of orthologous genes, including orthologous relationships of paralogous gene groups (Kanehisa et al., 2006).

In this framework, each gene is assigned a unique class of ortholog, often referred to as the K number, which serves as a crucial link between genes database resulting from the 16S-rRNA analysis with the pathway network information stored in the KEGG pathway database.
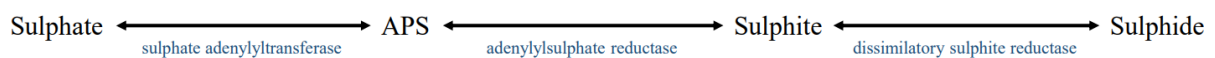
This approach has been validated as a highly effective means of establishing a coherent and comprehensive understanding of complex biological interactions.

The direct association of KO annotations with established pathways facilitates the concurrent identification of specific biochemical pathways, thereby shedding light on the potential degradation mechanisms inherent in the groundwater samples (Kanehisa et al., 2017).

In the context of this research, this approach serves as a pivotal tool to ascertain whether the sulphur and nitrate-reducing bacterial populations present at the study site are capable of effectively executing the metabolic processes necessary for the degradation of benzene. Specifically, methabolic pathway related to benzene degradation in the sulphur and nitrogen metabolism were first detected. Subsequently, based on the the abundance of the KO counts in the different samples, it was possible to hypothesize on the biodegradation activities in the area of investigation.

The sulphate-reducing bacteria, through the process of dissimilatory reduction, play a crucial role in transforming sulfur compounds into sulfide. These bacteria utilize various compounds as carbon sources and electron donors, such as benzene or phenol that can serve as substrates for these microorganisms (Rabus et al., 2013)

The dissimilatory sulphate reduction follows a well-defined pathway, each step facilitated by specific enzymes denoted below the reaction arrows below:

Sulphate $\longleftrightarrow$ APS $\longleftrightarrow$ Sulphite $\longleftrightarrow$ Sulphide

sulphate adenylyltransferase   adenylylsulphate reductase   dissimilatory sulphite reductase

Within this pathway, several KO identifiers play a significant role, and their presence is evaluated across the sampled piezometers. Although the microbes responsible for this pathway are present in all the piezometers, their abundance is specifically massive in P301, P302, and Pz12 (fig. 5.13). Notably, P302 stands out as the sample with substantial KO counts at each reaction step within the pathway.

Conversely, in P301 and Pz12, these KO identifiers are more concentrated in the reactions between adenosine 5'-phosphosulphate (APS) and sulfide. Intriguingly, in Pz20, a high presence of KO corresponding to the first reaction (sulphate to APS) is observed, suggesting that the dissimilatory sulphate reduction pathway is likely to be at a first stage in this piezometer.
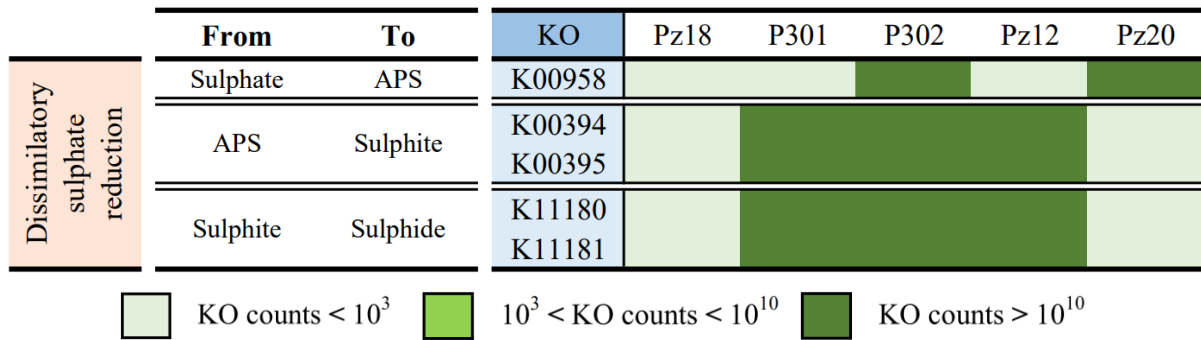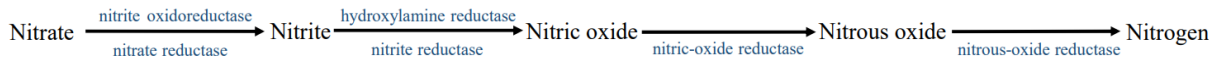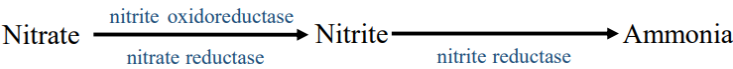
	From	**To**	**KO**	**Pz18**	**P301**	**P302**	**Pz12**	**Pz20**
Dissimilatory sulphate reduction	Sulphate	APS	K00958					
	APS	Sulphite	K00394 K00395					
	Sulphite	Sulphide	K11180 K11181					

☐ KO counts < 10^3 ☐ 10^3 < KO counts < 10^{10} ■ KO counts > 10^{10}

Fig. 5.13. KO identifiers counts involved in dissimilatory sulphate reduction in Bois Saint-Jean

With regards to the nitrogen metabolism, nitrate is an electron acceptor for cellular metabolism rather than for cell synthesis in both denitrification and dissimilatory nitrate reduction pathways (Ribeiro, et al., 2018). Denitrification represents a permanent nitrogen removal pathway by reducing nitrate to nitrogen (Tiedje, 1988):

Nitrate $\xrightarrow[\text{nitrate reductase}]{\text{nitrite oxidoreductase}}$ Nitrite $\xrightarrow[\text{nitrite reductase}]{\text{hydroxylamine reductase}}$ Nitric oxide $\xrightarrow{\text{nitric-oxide reductase}}$ Nitrous oxide $\xrightarrow{\text{nitrous-oxide reductase}}$ Nitrogen

Dissimilatory nitrate reduction is instead a nitrogen-conserving mechanism that transforms nitrate into another more bio-available inorganic-nitrogen form, ammonium (Tiedje, 1988):

Nitrate $\xrightarrow[\text{nitrate reductase}]{\text{nitrite oxidoreductase}}$ Nitrite $\xrightarrow{\text{nitrite reductase}}$ Ammonia

In a comparative analysis between the two degradation pathways, it becomes evident that denitrification exhibits relatively lower potential, as evidenced by the lower counts of KO identifiers associated with reactions from nitrite to nitrogen (fig. 5.14). Notably, this observation holds true for most piezometers, indicating a reduced prevalence of these reactions in the sampled groundwater. However, an interesting exception arises in Pz12, where a remarkably substantial count of KO identifiers is observed across the entire denitrification process, with a distinct presence in the reaction involving nitric oxide and nitrous oxide.

Furthermore, in Pz12 there also appears to be a potential for bacteria capable of performing dissimilatory nitrogen reduction. This potential, however, becomes more prominent in P301 and Pz18, where the counts of relevant KO identifiers are exceptionally high across the entirety of the dissimilatory nitrate reduction pathway. Conversely, in P302 and Pz20, while the presence of KO identifiers corresponding to different stages of the pathway is still detected, their overall counts are comparatively lower.

	From	To	KO	Pz18	P301	P302	Pz12	Pz20
Dissimilatory nitrogen reduction	Nitrate	Nitrite	K00370					
			K00371					
			K00374					
			K02567					
			K02568					
	Nitrite	Ammonia	K00362					
			K00363					
			K03385					
			K15876					
Denitrification	Nitrate	Nitrite	K00370					
			K00371					
			K00374					
			K02567					
			K02568					
	Nitrite	Nitric Oxide	K00368					
			K15864					
	Nitric oxide	Nitrous Oxide	K04561					
			K02305					
	Nitrous oxide	Nitrogen	K00376					

KO counts < 10^3 | 10^3 < KO counts < 10^{10} | KO counts > 10^{10}
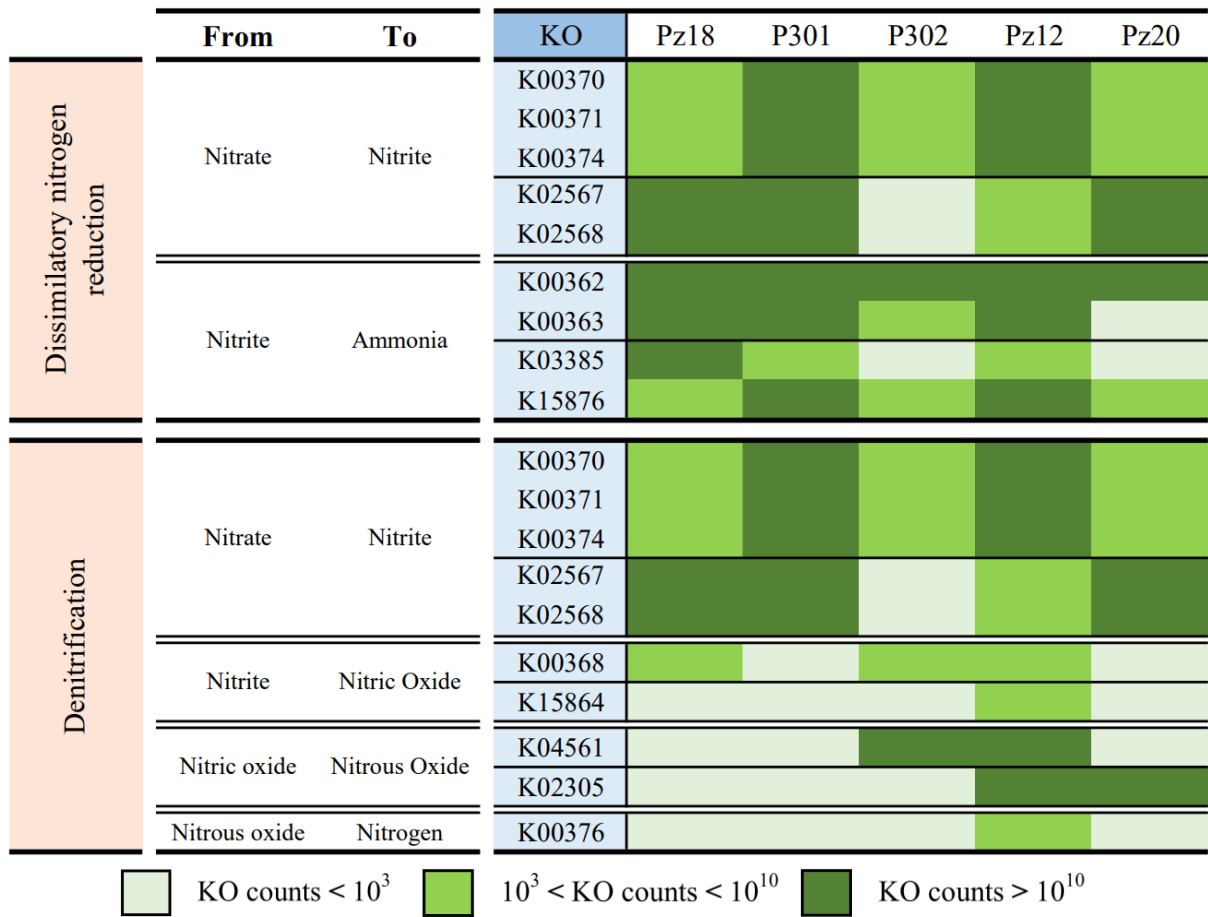
Fig. 5.14. KO identifiers counts involved in nitrogen reduction in Bois Saint-Jean

6. Discussion of the results

6.1. Differentiation of the areas of contamination

To comprehensively discuss the presented results, it is essential to distinguish the contaminated zones (P301, P302, and Pz18) from the areas that are either less contaminated or uncontaminated (Pz20 and Pz12). This division serves as a crucial framework for the ensuing discussion, allowing to explore distinct patterns and characteristics in the groundwater samples.

Notably, this discussion will solely focus on the groundwater, as the analysis of surface water from the Biez-du-Moulin river demonstrated an absence of pollutants. This partitioning becomes evident through various aspects of the results, where the contaminated zone exhibits unique attributes compared to the unaffected regions. This differentiation is particularly apparent in the microbial community structure as evidenced by the PCoA analysis, as well as in the hydrogeochemical diagrams and in the shared anoxic environment.

In the contaminated area, a notable reduction in benzene concentration over time stands out as a prominent feature. The analysis of benzene levels exhibited fluctuating trends during the sampling campaign before the implementation of the ISCO treatment on October 14, 2020. Subsequently, a substantial increase was observed on November 15, 2021, likely linked to the mobilization of trapped contaminants in the bedrock due to the push-pull experiment conducted in May 2021. Nevertheless, subsequent analyses revealed a consistent and progressive decline in benzene concentrations, indicating ongoing benzene degradation potentially attributed to both ISCO and microbial activities.

While all samples from the last analysis fall below the VS threshold stipulated by the 2018 Wallonia Soil Decree (10 µg/L), except for Pz18 (at 41 µg/L), it is imperative to avoid simplistic interpretations solely based on benzene concentrations when drawing conclusions about safety and degradation processes within the investigation site. Thus, the discussion delves into a multifaceted exploration employing various lines of evidence, including hydrogeochemical, isotopic, and microbial analyses.

The examination of the contaminated area can be further segmented into the source area (P301 and P302) and the plume area (Pz18), as these distinct zones present specific attributes and trends that contribute to a comprehensive understanding of the site's complex dynamics.

6.2. Source zone

The influence of the ISCO technique has deeply shaped the source area, leaving a marked impact on its hydrogeological dynamics. This is particularly evident in the case of P301 and P302, which played crucial roles as monitoring wells throughout the procedure. P301 was situated within the injection zone, while P302 is located downstream. The ISCO remediation process has imprinted distinct signatures within the area. Notably, the release of H^+ and CO_2 during the remediation has induced acidification, evident through lower pH levels in comparison to other samples. Additionally, considerable concentrations of sulphate in the area have been observed.

Both piezometers display a substantial reduction in benzene concentrations over time. For instance, P301 showed a decrease from 7500 µg/L in November 2021, to 1100 µg /L in July 2022, and ultimately to 7.90 µg/L in February 2023. This decline is likely due to a synergistic interplay between ISCO and microbial activities. To assess the potential for biodegradation, the push-pull test was conducted within these two piezometers as part of Hallberg's thesis research.

The BTC curves demonstrate potential degradation activities through nitrate reduction in the source area. This phenomenon is particularly evident in P301, where nitrate concentrations decreased over time even when corrected with the bromide dilution factor. The plausibility of biodegradation via nitrate reduction bacteria is further supported by the evolution of δ^{13}C-Bz isotopes, aligning with benzene degradation using nitrate as an electron acceptor in the computed enrichment factor.

Though denitrifying bacteria appear to be less abundant, there is compelling evidence of the presence of dissimilatory nitrogen reduction bacteria, as affirmed by the KO analysis. Notably, nitrate concentration in P301 falls below the detection limit, implying that the detected microbial community around P301 may stem from previous nitrate reduction conditions. The scarcity of nutrients might have prompted alternative pathways to develop.

The feasibility of benzene biodegradation through other electron acceptors gains support from the relatively higher presence of ferrous iron in P301 compared to the other piezometers. This suggests the possible involvement of ferric iron-reducing bacteria, which correlates with the measured redox potential on the field (E_h = -136.60). The concentration of ferrous iron has in fact increased from 300 µg/L in March 2021 to 8600 µg/L in February 2023, indicating a significant change over time.

Moreover, elevated methane concentrations in P301 hint at potential methanotrophic conditions that may have impacted the δ^{13}C-DIC in the piezometer. Regarding sulphate, the push-pull test did not yield conclusive evidence of biodegradation through sulphate reduction in the BTC analysis or through variations in δ^{34}S-SO$_4^{2-}$ and δ^{18}O-SO$_4^{2-}$. However, it is crucial to remember that these analyses may be not accurate due to various factors, such as the injection of sulphate tracer at a concentration similar to background levels and the not documented analytical approach considered for this study.

The inactivity of sulphate reducing bacteria in the push-pull test beside high sulphate concentration may be caused by microbial nitrate reduction, which produces nitrite as one intermediate, a strong inhibitor for dissimilatory sulphate reduction (Stoeva & Coates, 2019). Therefore, minor amounts of nitrate and its subsequent degradation product nitrite may stop the process of dissimilatory sulphate reduction in the aquifer (Müller et al., 2021).

Nevertheless, given the temporal context, the depletion of nitrate in P301 suggests that sulphate reduction could potentially have developed by 2023. This metabolic pathway is reinforced by the abundant dissimilatory sulphate-reducing bacteria as indicated by the KO analysis and the increase in δ^{34}S-SO$_4^{2-}$, coupled with a significant decrease in sulphate concentrations from 860 mg/L in March 2021 to 230 mg/L in February 2023.

Despite this evidence, the δ^{18}O-SO$_4^{2-}$, decrease is not in accordance with the δ^{34}S-SO$_4^{2-}$ increase, leading to a negative slope in the dual isotope ratio plot. This discrepancy can also be observed in P302 and has been documented not to deny sulphate reduction in certain conditions. In fact, other lines of evidence of dissimilatory sulphate reduction can be found for P302, as it shows an enrichment in δ^{34}S-SO$_4^{2-}$ with a decrease in normalized sulphate concentration, although to a lesser extent compared to P301.

Moreover, P302 showed potential sulphate reduction due to the enrichment of δ^{34}S-SO$_4^{2-}$ and δ^{18}O-SO$_4^{2-}$ in the push-pull test, even if no evidence could have been detectable from the BTC. Dissimilatory sulphate reduction is also plausible in this piezometer in light of the gradual increase in nitrate concentration, coupled with the limited evidence of denitrifying or dissimilatory nitrate-reducing bacteria.

The relatively low concentrations of methane and ferrous iron further suggest the absence of other significant microbial activities. Worth noting is the lack of substantial benzene concentration reduction in P302 over the past year, whereas significant decrease occurred from 1300 µg/L in November 2020 to 54 µg/L in March 2021.

The peak in ferrous concentration of 15000 µg/L in the March 2021 sampling campaign hints at the potential involvement of ferric iron-reducing bacteria in the observed drop during that time period.

6.3. Plume of contamination

The plume of contamination expands downgradient in the historically polluted piezometer Pz18, with a peak of 120000 µg/L in 2011. Over time, there was a gradual reduction in benzene concentrations within Pz18, eventually falling below the VS threshold in 2020. This decline can be attributed to contaminant volatilization and aquifer re-oxygenation following excavation activities in 2017. However, the execution of the push-pull experiment may have led to the remobilization of trapped benzene, causing its levels to rise again. Despite a gradual decrease since 2021, Pz18 remains the only well where benzene concentrations exceed the regulatory threshold set by the Wallonia Soil Decree.

Within this piezometer, robust evidence points towards microbial activity. Particularly convincing is the isotope analysis of $\delta^{15}N\text{-}NO_3^-$ and $\delta^{18}O\text{-}NO_3^-$, revealing substantial enrichments, although laboratory isotope analysis yielded faint signals due to nitrate concentrations falling below detection limits (< 0.90 mg/L) in the dataset provided by SPAQuE. However, major ion analyses performed by the University of Liège detected nitrate at 0.71 mg/L, supporting the possibility of biodegradation through nitrate-reducing bacteria.

This potential aligns with the well-evidenced dissimilatory nitrogen reduction highlighted in the KO analysis. Key nitrate-reducing bacteria, including those belonging to the Verrucomicrobiota and Nitrospira phyla, along with *Kaiserbacteria* from the Patescibacteria phylum, have been identified in the groundwater sampled from Pz18.

Furthermore, anaerobic biodegradation through alternative electron acceptors could be plausible, considering the relatively elevated levels of ferrous iron and methane, although to a lesser extent than in P301. The latter could have influenced the hydrogeochemistry of Pz18 being located hydrologically upgradient.

Additionally, biodegradation through sulphate-reducing bacteria is likely to occur in the area. This microbial pathway might have deployed as nitrate concentrations were too low to sustain nitrate-reducing bacterial activity. Despite the KO analysis indicating a relatively weak presence of dissimilatory sulphate-reducing bacteria, the dual isotope plot of $\delta^{34}S\text{-}SO_4^{2-}$ and $\delta^{18}O\text{-}SO_4^{2-}$ displays enrichments specific to Pz18. The correlation is supported by the increase

in $\delta^{34}S$-SO_4^{2-} coupled with the decrease in sulphate concentration, dropping from 750 mg/L in March 2021 to 480 mg/L in February 2023.

6.4. Peripheral area

Around the contaminated area, the focus turns to two distinct piezometers, Pz12 and Pz20. Pz12, previously considered as the reference for background concentrations, is located in close proximity to the source area. Meanwhile, Pz20 is positioned downstream of the contamination plume, situated between Pz18 and the surface water body, Biez-du-Moulin.

The reconsideration of Pz12 as the background reference has been questioned after careful examination of the detailed piezometric map within the investigation zone: by tracing the groundwater's flow direction as perpendicular to the piezometric curve, the possibility of contamination in Pz12 emerges. This suspicion was fortified by the results following the push-pull experiment conducted in March 2021. While benzene concentration in Pz12 (2.40 µg/L) remained below the detection limit during the other sampling campaigns, the isolated presence of benzene and a slight presence of toluene (0.54 µg/L), suggests the misconception in evaluating Pz12 as reflecting the background conditions.

Nevertheless, the hydrogeochemical characteristics of Pz12 markedly differ from those of the heavily contaminated areas, as it shows relatively high pH levels and detectable dissolved oxygen (0.99 mg/L). This divergence also extends to major ion composition, notably marked by nitrate presence at 11 mg/L and sulphate concentrations comparatively lower at 170 mg/L. Sulphate concentrations showed only a minor decrease since the March 2021 sampling campaign, where levels were measured at 200 mg/L.

Moreover, the dual isotope ratio plot of $\delta^{34}S$-SO_4^{2-} and $\delta^{18}O$-SO_4^{2-} revealed a positive shift, primarily attributed to an enrichment in $\delta^{18}O$-SO_4^{2-}, with minimal increases in the heavier sulphate isotope. Additionally, the nitrate isotopes present limited correlation between the relatively higher $\delta^{15}N$-NO_3^- compared to the $\delta^{18}O$-NO_3^- values.

In contrast, Pz20's $\delta^{15}N$-NO_3^- lower values show an opposite behaviour. Noteworthy is Pz20's well-oxygenated environment, as evidenced by its dissolved oxygen content of 4.73 mg/L. This context suggests that potential contaminants originating from the plume might experience accelerated aerobic degradation. Despite a benzene concentration of only 0.21 µg/L, Pz20 cannot be conclusively categorized as unpolluted, signifying that it might represent the outer boundary of the plume.

In terms of major ion composition, Pz20 show modest variation from Pz12. This consistency is mirrored in their graphical representation through Stiff and Piper diagrams. Unfortunately, direct comparisons with the March 2021 sampling campaign are precluded, as Pz20's analysis was integrated into this master's thesis sampling campaign, with the goal of delineating the plume's horizontal extension. However, $\delta^{34}S$-SO_4^{2-} and $\delta^{18}O$-SO_4^{2-} remarkably low value would exclude an enrichment in the heavier isotopes and thus degradation through sulphate reduction.

7. Conclusion and future perspectives

This study offers a valuable lens through which to unravel the intricate dynamics within zone 6 of Bois Saint Jean. The site's historical contamination and diverse remediation efforts have given rise to a complex correlation of factors. The core objective of this thesis is to determine whether the residual benzene contamination, though significantly reduced over the past decade, can be biodegraded by indigenous bacteria using a Monitored Natural Attenuation approach. To address this, a multifaceted analysis encompassing hydrogeochemical, isotopic, and microbial investigations was conducted. By integrating the results from the current sampling campaign with those from a previous master's thesis, which included slug and push-pull tests, a holistic perspective on intrinsic biodegradation potential emerges.

Although a clear indication of benzene degradation is evident, dissecting the exact mechanisms behind this process remains intricate. Unlike most research that interprets data under natural conditions, this site's unique challenge lies in its substantial influence from ISCO remediation, which complicates the interpretation of results. Nonetheless, the unmistakable signs of biodegradation are apparent from the analyses.

Notably, within the source area, P301 exhibits evidence of possible dissimilatory nitrogen reduction, ferric iron reduction, and potentially even dissimilatory sulphate-reducing bacteria activity. P302, on the other hand, more convincingly points toward dissimilatory sulphate reduction, with limited evidence of other significant microbial processes.

Pz18, located in the plume and characterized by benzene levels higher than VS threshold, demonstrates clear isotopic and microbial signals associated with dissimilatory nitrate reduction. However, the presence of potentially inhibitory sulphate-reducing bacteria is also assessed even if, in theory, their activity should be inhibited by nitrate-reducing bacteria.

Pz12, initially considered uncontaminated, hints at potential impact from groundwater flow. Pz20, which could be regarded as the plume's edge, displays slight presence of benzene. However, neither piezometer demonstrates substantial biodegradation potential, and the presence of dissolved oxygen suggests that aerobic bacteria might eventually degrade trace amounts of benzene.

The discussion highlights the challenge of achieving coherence among the diverse lines of evidence, thus complicating the establishment of a definitive conclusion.

As anticipated by this study, the inclusion of a reference background piezometer proves pivotal in facilitating comparisons and detecting variations indicative of microbial activity. Expanding the piezometer network within the area would enhance data comprehensibility by capturing a broader range of variations and would enhance the current limited reliability of microbial analysis results.

An improved approach to understanding contamination plume evolution could involve the installation of additional piezometers between the source area and Pz18, and between Pz18 and the downgradient Pz20. This would provide a more comprehensive representation of the plume's spatial variability and evolution over time.

Moreover, the temporal evolution of results becomes a key insight. The analysis of benzene evolution offers invaluable data for tracing changes over time. However, the nitrate and carbon isotope results, exclusively analysed during the last sampling campaign, preclude precise conclusions. While the analysis of sulphate isotopes from two sampling campaigns aids in understanding evolution, the data set remains incomplete, necessitating further investigation of sulphate isotope interpretation.

Temporal evolution gains particular significance in microbial analysis, where the static nature of the data contrasts with the dynamic nature of microbial communities. The comparison of these communities over time holds the potential to unveil stability or fluctuations influenced by temporary factors.

In addition, the implementation of a high-flow sampling procedure for the push-pull experiment has raised questions about the reliability of the conventional low-flow technique commonly employed in site investigations. This is evident in the significant variance in benzene concentrations between the two methods. While the high-flow approach reveals higher benzene concentrations, potentially reflecting trapped contaminants, the low-flow technique may fail to capture their presence, leading to an underestimation of true contamination levels.

The insights gleaned from these analyses collectively underscore the intricate nature of data interpretation within a dynamic and evolving subsurface environment. Results indicate the sulphate-reducing conditions seem to occur in the aquifer, although not robust enough to ensure Monitored Natural Attenuation based on dissimilatory sulphate reduction is a safe option.

On the other hand, consistently across both the previous study conducted in Hallberg's thesis in 2021 and the current investigation, the most compelling evidence indicates biodegradation through nitrate reduction, particularly via the dissimilatory nitrate reduction pathway.

However, the low concentration of nitrate present in the contaminated area raises concerns about the feasibility of relying solely on monitored natural attenuation to effectively reduce contamination levels below the established VS threshold in a stable manner.

To address this challenge, an enhanced bioremediation approach involving bio-stimulation through the injection of supplementary nutrients containing nitrate emerges as a potential solution. Such an approach could foster the growth of indigenous microorganisms, leading to an increase in their population and thereby promoting the degradation of benzene within the system.

References

Ahad, J., Sherwood, B., Edwards, E., Slater, G., & Sleep, B. (2000). Carbon isotope fractionation during anaerobic biodegradation of toluene: Implications for intrinsic bioremediation. *Environ. Sci. Technol.*, 34:892-896.

Alvarez-Rogel, J., Penalver, A. A., Jiménez-Càrceles, F., Tercero, M., & Nazaret, G.-A. (2021). Evidence supporting the value of spontaneous vegetation for phytomanagement of soil ecosystem functions in abandoned metal(loid) mine tailings. *Catena*, 201:105-191.

Alzarez, P., & Illman, W. (2006). Bioremediation and Natural Attenuation: Process Fundamentals and Mathematical Models. *Willey Interscience.* New York.

Antler, Antler, G., Turchyn, A., Rennie, V., Herut, B., & Sivan, O. (2013). Coupled sulfur and oxygen isotope insight into bacterial sulphate reduction in the natural environment. *Geochemica et Cosmochimica, Vol. 118*, 98-117.

Appelo, C., & Postma, D. (2010). *Geochemistry, Groundwater and Pollution.* CRC Press - Taylor & Francis Group.

Balland-Bolou-Bi, C., Brondeau, F., & Jusselme, M. (2022). Can Natural Attenuation be Considered as an Effective Solution for Soil Remediation? *IntechOpen: Soil Contamination - Recent Advances and Future Perspectives*.

Beck, P., & Mann, B. (2010). A technical guide for demonstrating monitored natural attenutation of petroleum hydrocarbons in groundwater. *CRC - No. 15 Technical Report*.

Beller, H., Kane, S., Legler, T., & Alvarez, P. (2002). A Real-Time Polymerase Chain Reaction Method for Monitoring Anaerobic, Hydrocarbon-Degrading Bacteria Based on a Catabolic Gene. *Environ. Sci. Technol.*, 36, 18, 3977-3984.

Bergmann, F., Nidal, M., Laban, A., Meyer, A., Elsner, M., & Meckenstock, R. (2011). Dual (C, H) Isotope Fractionation in Anaerobic Low Molecular Weight (Poly)aromatic Hydrocarbon (PAH) Degradation: Potential for Field Studies and Mechanistic Implications. *Environmental Science & Technology*, 45, 6947-6953.

Bigeleisen, J., & Wolfsberg, M. (1959). Theoretical and experimental aspects of isotope effects in chemical kinetics. *Adv. Chem. Phys.*, 1:15-76.

Borden, R., Gomez, C., & Becker, M. (2000). Geochemical indicators of intrinsic bioremediation. *Ground Water*, 33:180-189.

Burbery, L., Cassiani, G., Andreotti, G., Ricchiuto, T., & Semple, K. (2004). Single-well reactive tracer test and stable isotope analysis for determination of microbial activity in a fast hydrocarbon-contaminated aquifer. *Environmental Pollution, vol. 129*, 321-330.

Cao, Y., Yu, M., Dong, G., & Chen, B. (2020). Digital PCR as an Emerging Tool for Monitoring of Microbial Biodegradation. *Molecules*, 25(3):706.

Carey, M., Finnamore, J., Marslands, P., & Morrey, M. (2000). Guidance on the Assessment and Monitoring of Natural Attenuation of Contaminants in Groundwater. *Envrionment Agency.* Bristol: R&D Pibòo.

Casciotti, K., Buchwald, C., Santoro, A., & Frame, C. (2011). Assessment of nitrogen and oxygen isotopic fractionation during nitrification and its expression in the marine environment. *Methods in Enzimology*, pp. 253-280.

Castro, R., Avila, J. P., Ye, M., & Sansores, A. (2018). Groundwater Quality: Analysis of Its Temporal and Spatial Variability in a Karst Aquifer. *Groundwater Vol. 56*, 62-72.

Chatterjee, S., Dickens, G., Bhatnagar, G., Chapman, W., Dugan, B., Snyder, G., & Hirasaki, G. (2011). Pore water sulfate, alkalinity, and carbon isotope profiles in shallow sediment above marine gas hydrate systems: A numerical modeling perspective. *Journal of Geophysical Research: Solid Earth, Vol. 116.*

Collin, P. (2001). *Dictionary of Ecology and the Environment.* London: Peter Collin Publishing.

Davis, G., Barber, C., Power, R., Thierrin, J., Patters, B., & Wu, Q. (1999). The variability and intrinsic remediation of a BTEX plume in anaerobic sulphate-rich groundwater. *J. Contam.*, 36:265-290.

Declercq, I., Cappuyns, V., & Duclos, Y. (2012). Monitored natural attenuation (MNA) of contaminated soils: State of the art in Europe - A critical evaluation. *Science of the Total Environment 426*, 393 - 405.

Deutsh, W. (1997). Groundwater Chemsitry: Fundamentals and Applications to Contamination. *CRC Press - Taylor & Francis Group.*

ECOREM. (2000). *Mission d'expertise du site Bois St-Jean à Ougrée, Etude de l'état actuel.* Mechelen.

EPRI. (2004). *A Review of Monitored Natural Attenuation Remedy for Manufactured Gas Plant Sites.* Palo Alto, CA: Electric Power Research Institute.

Fahy, A., McGenity, T., Timmis, K., & Ball, A. (2006). Heterogeneous aerobic benzene-degrading communities in oxygen-depleted groundwaters. *FEMS Microbiology Ecology*, Volume 58, Issue 2.

Feisthauer, S., Seidel, M., Bombach, P., Traube, S., Knoeller, K., Wange, M., . . . Richnow, H. (2012). Characterization of the relationship between microbial degradation processes at a hydrocarbon contaminated site using isotopic methods. *Journal of Contaminant Hydrology, vol. 133*, 17-29.

Field, J. (2002). Limits of anaerobic biodegradation. *Water Sci Technol*, 45(10):9-18.

Granger, J., Sigman, D., Lehmann, M., & Tortell, P. (2008). Nitrogen and oxygen isotope fractionation during dissimilatory nitrate reduction by denitryfing bacteria. *Oceanogr. 53(6)*, 2533-2545.

Halen, H., Moutier, M., Beuthe, B., Namèche, T., Vounaki, O., & Nuyens, D. (2010). *Rapport de l'évaluation finale – Cahier des bonnes pratiques no. 9.* Liège: SPAQuE.

Hallberg, K. S. (2021). *Master's thesis: Evidencing biodegradation of organic pollutants using push-pull tracer experiments.* University of Liège: Faculty of Applied Science.

Huang, Y., Wang, Y., Feng, H., Jianghuai, W., Yang, X., & Wang, Z. (2019). Genome-guided identification and characterization of bacteria for simultaneous degradation of polycyclic aromatic hydrocarbons and resistance to hexavalent chromium. *International Biodeterioration & Biodegradation*, 138:78-86.

Istok, J. (2013). Push-Pull Tests for Size Characterization. In *Lecture Notes in Earth System Sciences.* Springer.

Kanehisa, M., Furumichi, M., Tamane, M., Sato, Y., & Morishima, K. (2017). KEGG: new perspectives on genomes, pathways, diseases and drugs. *Nucleic Acids Research, Vol. 45*, 353–361.

Kanehisa, M., Goto, S., Hattori, M., Aoki-Kinoshita, K., Itoh, M., Kawashima, S., . . . Hirakawa, M. (2006). From genomics to chemical genomics: new developments in KEGG. *Nucleic Acids Research, Vol. 34*, 354–357.

Kanwartej, S., Ponsin, V., Kolhatkar, R., Hunkeler, D., Thomson, N., Madsen, E., & Buscheck, T. (2022). Sulfate Land Application Enhances Biodegradation in a Petroleum Hydrocarbon Smear Zone. *Groundwater Monitoring & Remediation, Vol. 43*, 44-59.

Kao, C., Chien, H., Surampalli, R., Chien, C., & Chen, C. (2010). Assessing of Natural Attenuation and Intrinsic Bioremediation Rates at a Petroleum-Hydrocarbon Spill Site: Laboratory and Field Studies. *Journal of Environmental Engineering*, 54-69.

Keller, A., Kleinsteuber, S., & Vogt, C. (2018). Anaerobic Benzene Mineralization by Nitrate-Reducing and Sulfate-Reducing Microbial Consortia Enriched From the Same Site: Comparison of Community Composition and Degradation Characteristics. *Microbial Ecology*, 75, 941-953.

Kennedy, L., Everett, J., Dewers, T., Pickins, W., & Edwards, D. (1999). Application of mineral iron and sulphide analysis to evaluate natural attenuation at fuel contaminated site. *J. Environ. Eng.*, 125:47-56.

Key, T., Sorsby, S., Wang, Y., & Madison, A. (2022). Framework for field-scale application of molecular biological tools to support natural and enhanced bioremediation. *Frontiers in Microbiology*, Vol. 13.

Kleikemper, J., Schroth, M., Sigler, W., Schmucki, M., Bernasconi, S., & Zeyer, J. (2002). Activity and Diversity of Sulfate-Reducing Bacteria in a Petroleum Hydrocarbon-Contaminated Aquifer. *Applied and Environmental Microbiology*, p. 1516-1523.

Kleikemper, J., Schroth, M., Sigler, W., Schmucki, M., Bernasconi, S., & Zeyer, J. (2002). Activity and Diversity of Sulfate-Reducing Bacteria in a Petroleum Hydrocarbon-Contaminated Aquifer. *Applied and Environmental Microbiology*, 1516-1523.

Kliushnikova, T., Chernyshenko, D., & Kasatkina, T. (1992). The sulfate-reducing capacity of bacteria in the genus Pseudomonas. *Mikrobiol Zh*, 54(2):49-54.

Knierim, K., Pollock, E., Hays, P., & Khojasteh, J. (2015). Using stable isotopes of carbon to investigate the seasonal variation of carbon transfer in northwestern Arkansas Cave. *Journal of Cave and Karst Studies, Vol. 77*, 12-27.

Knöller, K., Vogt, C., Richnow, H., & Weise, S. (2006). Sulfur and Oxygen Isotope Fractionation during Benzene, Toluene, Ethyl-Benzene and Xylene Degradation by Sulfate-Reducing Bacteria. *Environ. Sci. Technol., Vol. 40*, 3879-3885.

Lee, J.-Y., Cheon, J.-Y., Lee, K.-K., Lee, S.-Y., & Lee, M.-H. (2001). Statistical Evaluation of Geochemical Parameter Distribution in a Ground Water System Contaminated with Petroleum Hydrocarbon. *J. Environ. Qual. *, Vol. 30.

Liang, S., Kao, C., Kuo, Y., Chen, K., & Yang, B. (2011). In situ oxidation of petroleum-hydrocarbon contaminated groundwater using passive ISCO system. *Water Research*, 45:2496-2506.

Lollar, B., Slater, G., Sleep, B., Witt, M., Klecka, G., Harkness, M., & Spivack, J. (2001). Stable carbon isotope evidence for intrinsic bioremediation of tetrachloroethene and trichloroethene at area 6. *Environ. Sci. Technol.*, 35(2), 261 - 269.

Lox, A. (2023). *Rapport de caractérisation: Site de Bois Saint-Jean à Ougrée.* Liège: SPAQuE.

Mancini, S., Ulrich, A., Lacrampe-Couloume, G., Sleep, B., Edwards, E., & Sherwood, B. (2003). Carbon and hydrogen isotopic fractionation during anaerobic biodegradation of benzene. *Appl. Environ. Microbiol.*, 69:191-198.

Mariotti, A., Germon, J., Hubert, P., Kaiser, P., Letolle, R., Tardieux, A., & Tardieux, P. (1981). Experimental determination of nitrogen kinetic isotope fractionation - Some principles - Illustration for the denitrification and nitrification process. *Plant Soil*, 62:413-430.

McBurnett, L., Holt, N., Alum, A., & Abbaszadegan, M. (2018). Legionella - A threat to groundwater: Pathogen transport in recharge basin. *Science of The Total Environment, Volume 621*, 1485-1490.

Meckenstock, R. M. (2004). Stable isotope fraction analysis as a toll to monitor biodegradation in contaminated aquifers. *Journal of Contaminant Hydrology*, Vol. 75; pp 215-225.

Mengyuan, J., Lurui, X., Usman, M., Liu, C., Treu, L., Campanaro, S., & Luo, G. (2023). Different microplastics in anaerobic paddy soils: Altering methane emissions by influencing organic matter composition and microbial metabolic pathways. *Chemical Engineering Journal*, Vol 469.

Mohammadi, S., & Prasanna, B. (2003). Analysis of Genetic Diversity in Crop Plants—Salient Statistical Tools and Considerations. *Crop Science, Vol. 43*, 1234-1248.

Mohareb, S., Ben-aazza, S., Hadfi, A., El House, M., Karmal, I., Belattar, M., . . . Driouiche, A. (2021). Geochemical and thermodynamic study about the transport pipes clogging of treated wastewater and sprinklers of Agadir Golf Ocean, Southern Morocco. *Nanotechnology for Environmental Technology*, 43.

Morasch, B., Richnowh, Schink, B., Vieth, A., & Meckenstock, R. (2002). Carbon and hydrogen stable isotope fractionation during aerobic bacterial degradation of aromatic hydrocarbons. *Appl. Environ. Microbiol.*, 68:5191-5194.

Müller, C., Knoller, K., Lucas, R., Kleinsteuber, S., Trabitzsch, R., Weibs, H., . . . Vogt, C. (2021). Benzene degradation in contaminated aquifers: Enhancing natural attenuation by injecting nitrate. *Journal of Contaminant Hydrology, Vol. 238*.

Pandolfo, E., Caracciolo, A., & Rolando, L. (2023). Recent Advances in Bacterial Degradation of Hydrocarbons. *Water*, 13, 375.

Pankrantz, T. (2001). *Environmental Engineering Dictionary and Directory.* Boca Raton, FL: CRC Press.

Penton, C., Johnson, T., Quensen III, J., Iwai, S., & Cole, J. (2013). Functional genes to assess nitrogen cycling and aromatic hydrocarbon degradation: primers and processing matter. *Front. Microbiol.*, Vol. 4.

Puls, R. W., & Barcelona, M. J. (1995). *Low-flow (Minimal Drawdown) Groundwater Sampling.* United States Environmental Protection Agency, Office of Research and Development.

Quay, P., Emerson, S., & Devol, A. (1986). The carbon cycle for Lake Washington - A stable isotope study. *Limnol. Oceanogr. 31(3)*, 596-611.

Rabus, R., Hansen, T., & Widdel, F. (2013). Dissimilatory Sulfate- and Sulfur-Reducing Prokaryotes. *The Prokaryotes*.

Rees, C. (1973). A steady-state model for sulphur isotope fractionation in bacterial reduction processes. *Geochim. Cosmochim. Acta, Vol. 37*, 1141-1162.

Regenesis. (2018). *Regenesis.com.* Retrieved from PersulfOX Achieves Rapid Closure for a 30-Year Open LUST Case: https://regenesis.com/en/remediation-products/persulfox-persulfox-sp/

Remmani, R., Makhloufi, R., Miladi, M., Adbelkader, O., Canales, A. R., & Dàmaris, N.-G. (2021). Development of Low-Cost Activated Carbon towards an Eco-Efficient Removal of Organic Pollutants from Oily Wastewater. *Pol. J. Environ. Stud. Vol. 30 N.2*, 1-8.

Ribeiro, H., de Sousa, T., Santos, J., Sousa, A., Teixeira, C., Monteiro, M., . . . Magalhaes, C. (2018). Potential of dissimilatory nitrate reduction pathways in polycyclic aromatic hydrocarbon degradation. *Chemosphere, Vol. 199*, 54-67.

Rohlf, F. (1972). An empirical comparison of three ordination techniques in numerical taxonomy. *Syst. Zool., Vol. 21*, 271-280.

Ruthy, I., Willems, T., & Dassargues, A. (2016). *Carte Hydrogèologique de Wallonie, Seraing-Chenée 42/5-6.* Université de Liège: Service Public de Wallonie (SPW).

Ryu, H., & Cho, K. (2012). Characterization of the Bacterial Community in a Biocover for the Removal of Methane, Benzene and Toluene. *Microbiology and Biotechnology Letters - Vol. 40,*, 76-81.

Sarkar, D., Ferguson, M., Datta, R., & Birnbaum, S. (2004). Bioremediation of petroleum hydrocarbons in contaminated soils: Comparison of biosolids addition, carbon supplementation, and monitored natural attenuation. *Environ Pollut. 2005 Jul*, 136(1):187-95.

Sasamoto, H., Mikazu, Y., & Arthur, R. (2007). Estimation of in situ groundwater chemistry using geochemical modeling: A test case for saline type groundwater in argillaceous rock. *Physics and Chemistry of the Earth*, Vol. 32, 196-208.

Schroth, M., Kleikemper, J., Bolliger, C., Bernasconi, S., & Zeyer, J. (2001). In situ assessment of microbial sulfate reduction in a petroleum-contaminated aquifer using push–pull tests and stable sulfur isotope analyses. *Journal of Contaminant Hydrology, vol. 51*, 179-195.

Scroth, M. H., Kleikemper, J., Bolliger, C., Bernasconi, S. M., & Zeyer, J. (2001). In situ assessment of microbial sulfate reduction in a petroleum-contaminated aquifer using push–pull tests and stable sulfur isotope analyses. *Journal of Contaminant Hydrology 51*, 179-195.

Seagren, E., & Becker, J. (2002). Review of Natural Attenuation of BTEX and MTBE in Groundwater. *Practice Periodial of Hazardous, Toxic and Radioactive Waste Management*.

Service Public de Wallonie (SPW). (1er Mars 2018). *Décret relatif à la gestion et à l'assainissement des sols.* Region Wallonie: [C − 2018/70014].

Service public de Wallonie (SPW). (2008). *Guide de Référence pour le project d'assainissement.* Code Wallon de Bonnes Pratique V05.

Sevee, J. E., White, C. A., & Maher, D. J. (2000). An Analysis of Low-Flow Groundwater Sampling Methodology. *Ground Water Monitoring and Remediation*, 20(2):87-93.

Simler, R. (2012). *Tutoriel pour DIAGRAMMES.* Retrieved from Laboratoire d'Hydrogéologie d'Avignon.

Sinke, A. (2001). Monitored natural attenuation; moving forward to consensus. *Land Contamination and Reclamation, 9*, No. 1, 111-118.

Slater, G., Ahad, J., Lollar, B., Allen-King, R., & Sleep, B. (2000). Carbon isotope effects resulting from equilibrium sorption of dissolved VOCs. *Anal. Chem.*, 72 (22), 5669-5672.

Smith, M., Parker, S., Gammons, C., Poulson, S., & Hauer, F. (2011). Tracing dissolved O2 and dissolved inorganic carbon stable isotope dynamics in the nyack aquifer: middle Fork Flathead River, Montana, USA. *Geochim. Cosmochim. Acta, Vol. 75*, pp. 5971-5986.

SPAQuE. (2003). *Etude Hydrogeologique - Site D'activite Economique Desaffecte, Boin Saint Jean (Ougrée).* Liège.

SPAQuE. (2006). *"Bois Saint Jean" - Rapport de réhabilitation.* Liège.

SPAQuE. (2017). *Campagne d'investigations complémentaires dans la zone sud-ouest du site "Bois St-Jean".* Liège.

SPAQuE. (2017). *Etat des connaiscences à l'issue du project d'assainissement de la zone contaminée en benzène (LG6303-001 - "Bois Saint-Jean").* Liège.

SPAQuE. (2020). *Bois Saint-Jean.* Retrieved from SPAQuE: https://spaque.be/realisations/bois-saint-jean/

SPAQuE. (2022). *Lg6503-001 - Site "Bois Saint-Jean", Bilan Historique des Activités.* Liège.

Stoeva, K., & Coates, D. (2019). Specific inhibitors of respiratory sulfate reduction: towards a mechanicistic understanding. *Microbiology, Vol. 165*, 254-269.

Suez. (2020). *PAQ 6.1 Traitement de la nappe phreatique - Procedure.* Industrial Waste Specialties, Soil remediation.

Thornton, S., & Rivett, M. (2008). Monitored natural attenuation of organic contaminants in groundwater: Principles and application. *Water Management*, 161(6):381-392.

Thornton, S., Quigley, S., Spence, M., Banwart, S., Bottrell, S., & Lerner, D. (2001). Processes controlling the distribution and natural attenuation of dissolved phenolic compounds in a deep sandstone aquifer. *Journal of Contaminant Hydrology*, 53, No. 3–4, 233–267.

Tiedje, J. (1988). Ecology of denitrification and dissimilatory nitrate reduction to ammonium. *Biology of Anaerobic Microorganisms*, 179-244.

Toumi, M., Abbaszade, G., Sbaoui, Y., Farkas, R., Acs, E., Jurecska, L., & Toth, E. (2021). Cultivation and Molecular Studies to Reveal the Microbial Communities of Groundwaters Discharge Located in Hungary. *Water, Vol. 13*.

United States Environmental Protection Agency. (1999). *Use of Monitored Natural Attenuation at Superfund, RCRA Corrective Action and Underground Storage Tank Sites.* Washington, DC: USEPA.

Vieth, A., Kastner, M., Schirmer, M., Weibs, H., Godeke, S., Meckenstock, R., & Richnow, H. (2005). Monitoring In Situ Biodegradation of Benzene and Toluene by Stable Carbon Isotope Fractionation. *Environmental Toxicology and Chemistry*, Vol. 24, No.1, pp- 51-60.

Ward, J., Ahad, J., Lacrampe-Couloume, G., Slater, G., Edawrds, E., & Sherwood, B. (2000). Hydrogen isotope fractionation during methanogenic degradation of toluene: Potential for direct verification of bioremediation. *Environ. Sci. Technol.*, 34:4577-4581.

Weisse, L., Héchard, Y., Moumen, B., & Delafont, V. (2022). Here, there and everywhere: Ecology and biology of the Dependentiae phylum. *Environmental Microbiology*, Vol. 23, p. 597-605.

Wiedemeier, T., Rifai, H., Newell, C., & Wilson, J. (1999). *Natural Attenuation of Fuels and Chlorinated Solvents in the Subsurface.* New York: Wiley.

Yang, L., Yongjun, L., Zhang, A., Liu, Z., Yang, Z., Wei, C., & Li, Z. (2023). Cumulative effects and metabolic characteristics of aromatic compounds in microbial cells during the biochemical treatment process of coal chemical wastewater. *Chemical Engineering Journal*, Vol. 471.